PENNSTATE

1855

Design and Discovery using Material Modeling Methods

Susan B. Sinnott
Department of Materials Science and Engineering
Penn State University
University Park, PA

DEPARTMENT OF
MATERIALS SCIENCE AND ENGINEERING
COLLEGE OF EARTH AND MINERAL SCIENCES

MXene Synthesis *in silico*

Michael Ashton[1], Kiran Matthew[2], Richard Hennig[1], and Susan B. Sinnott[3]
Department of Materials Science and Engineering
[1]University of Florida
[2]Cornell University
[3]Penn State University

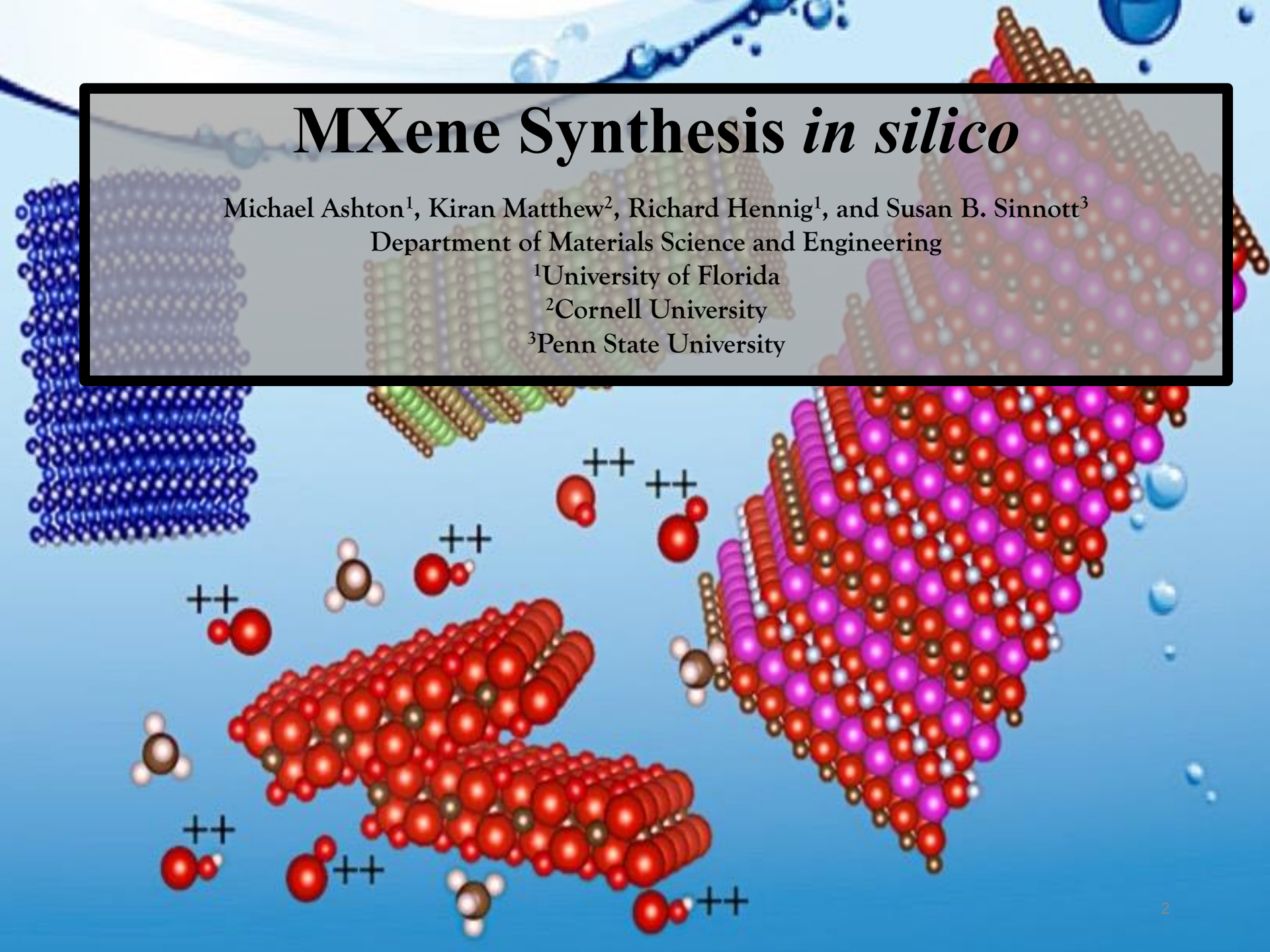

MAX Phase stability

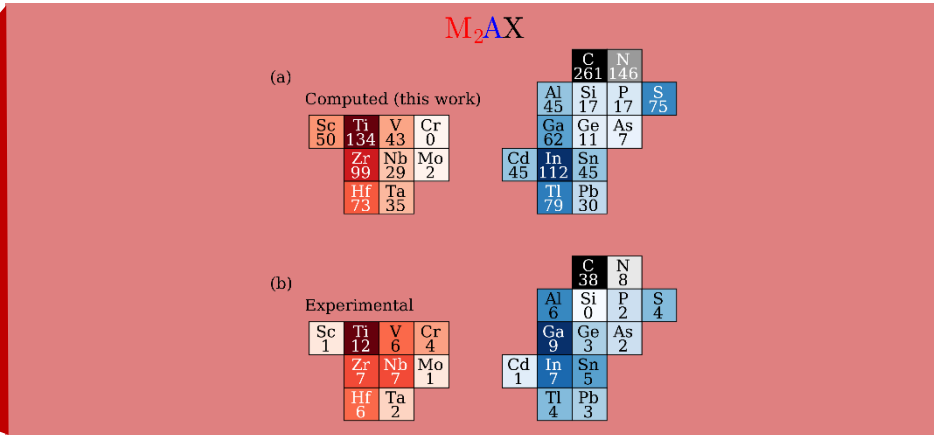

MXene stability

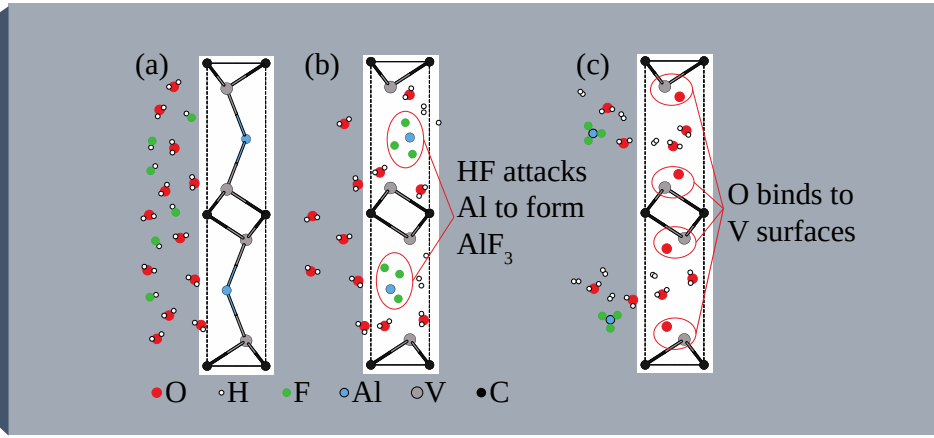

MXenes as LIB anodes

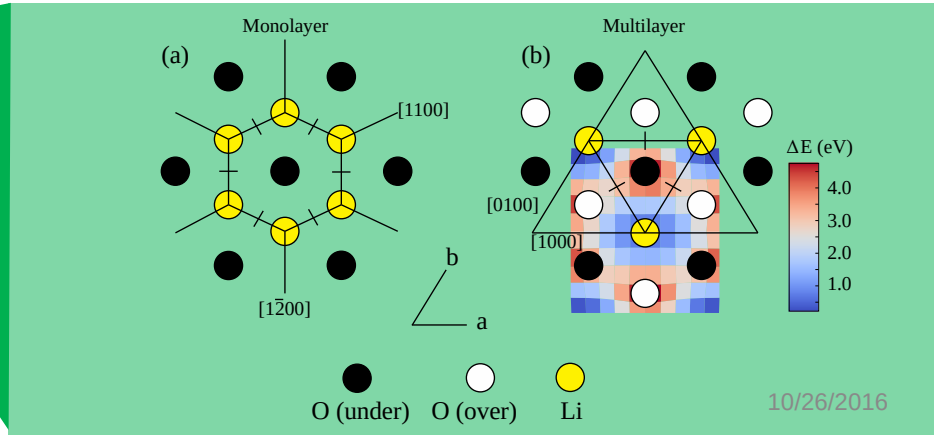

10/26/2016

MAX Phase stability

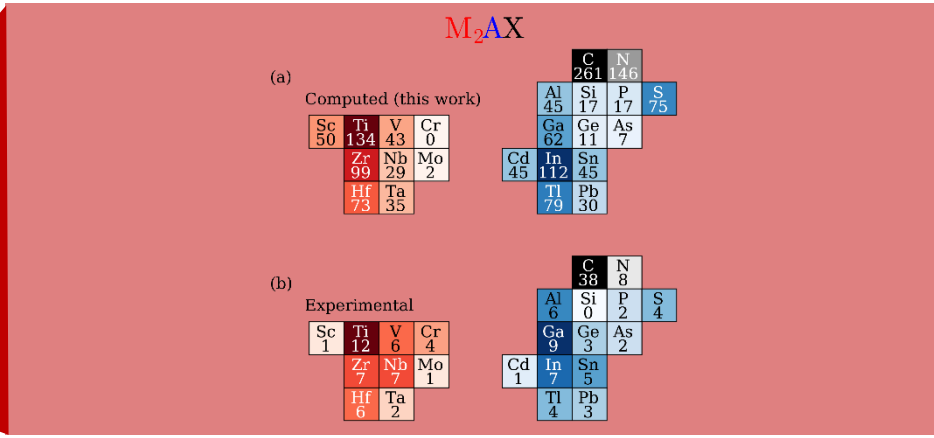

MXene stability

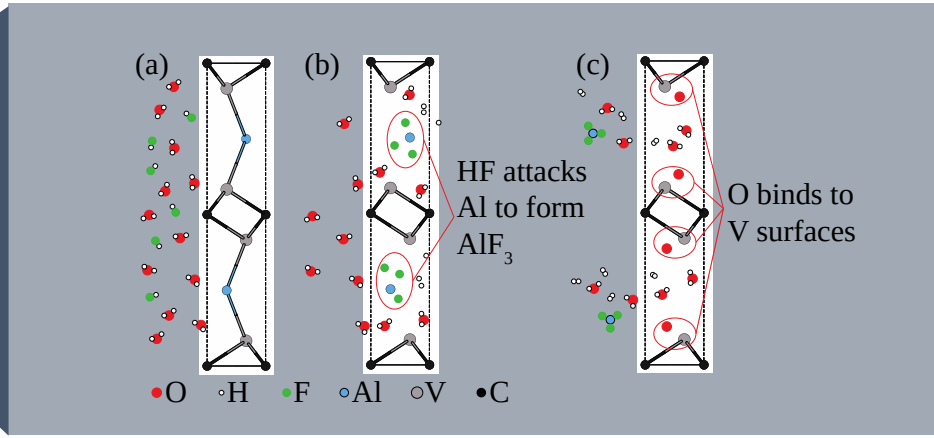

MXenes as LIB anodes

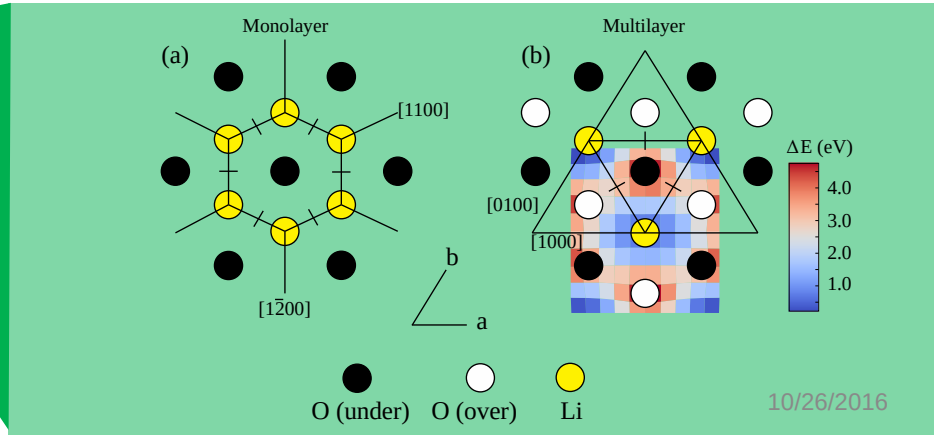

10/26/2016

MAX Phases

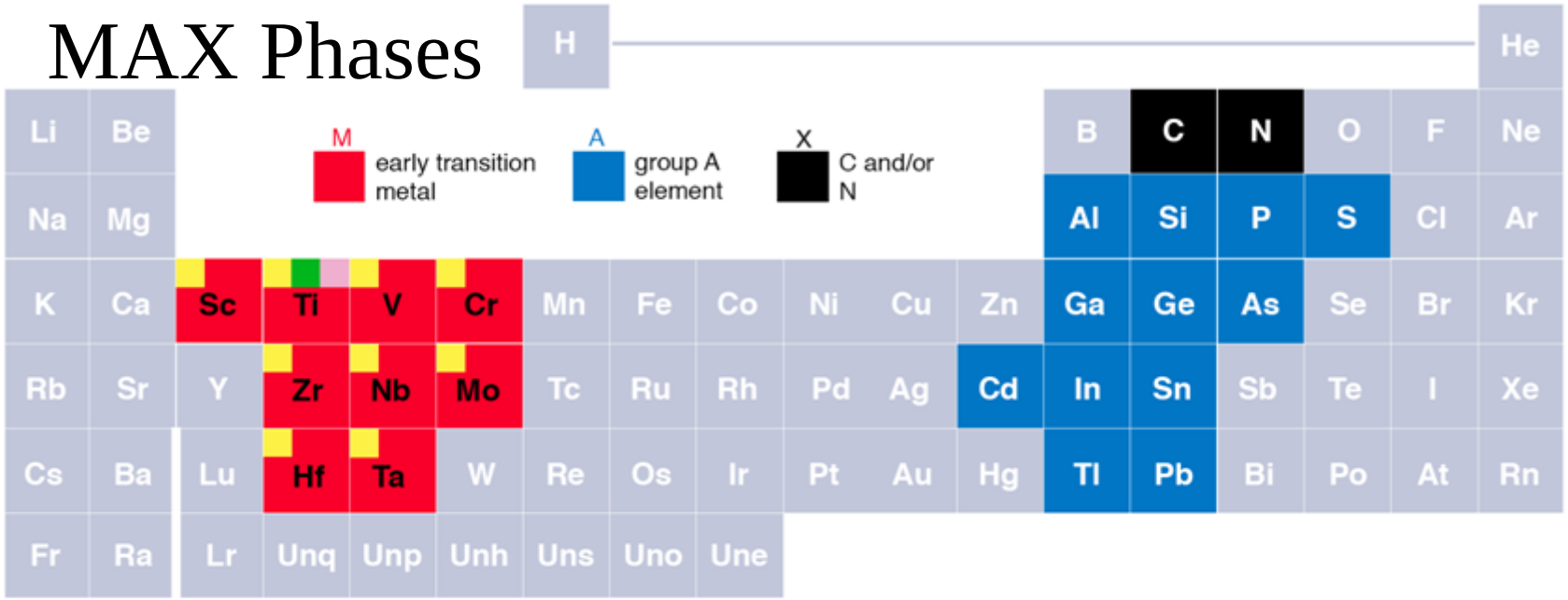

9 ***M*** elements
× 12 ***A*** elements
× 2 ***X*** elements
× 3 values of *n*

648 MAX phases

50/50 solid solutions also possible for ***M***, ***A***, and ***X***

31,590 MAX phases

(10,530 M_2AX phases)

MAX Phase Applications

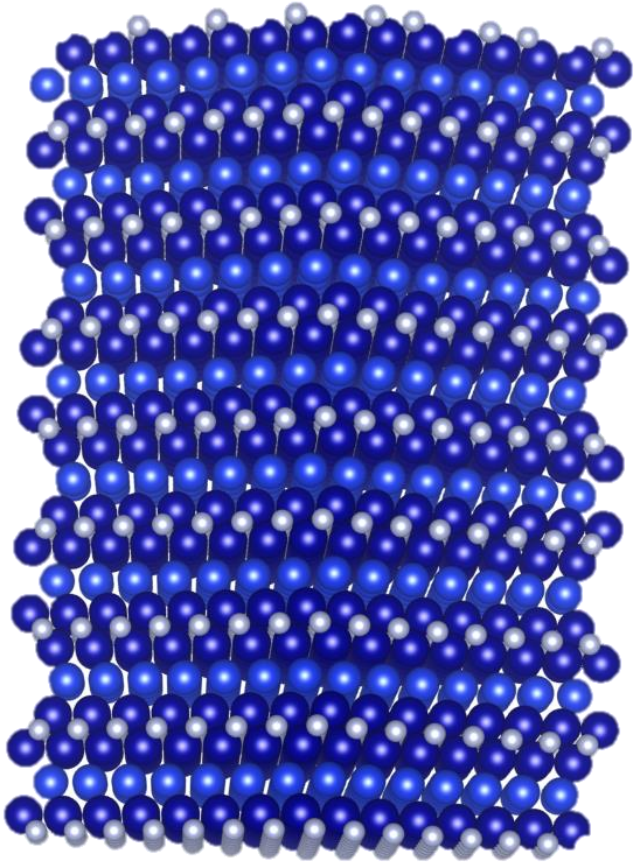

- High-T coatings
- Low friction coatings
- Impact-absorption coatings
- Heating elements
- Electrical contacts
- Radiation cladding
- Machinable magnets
- Precursors for *MXenes*

Thermodynamic stability of M_2AX phases

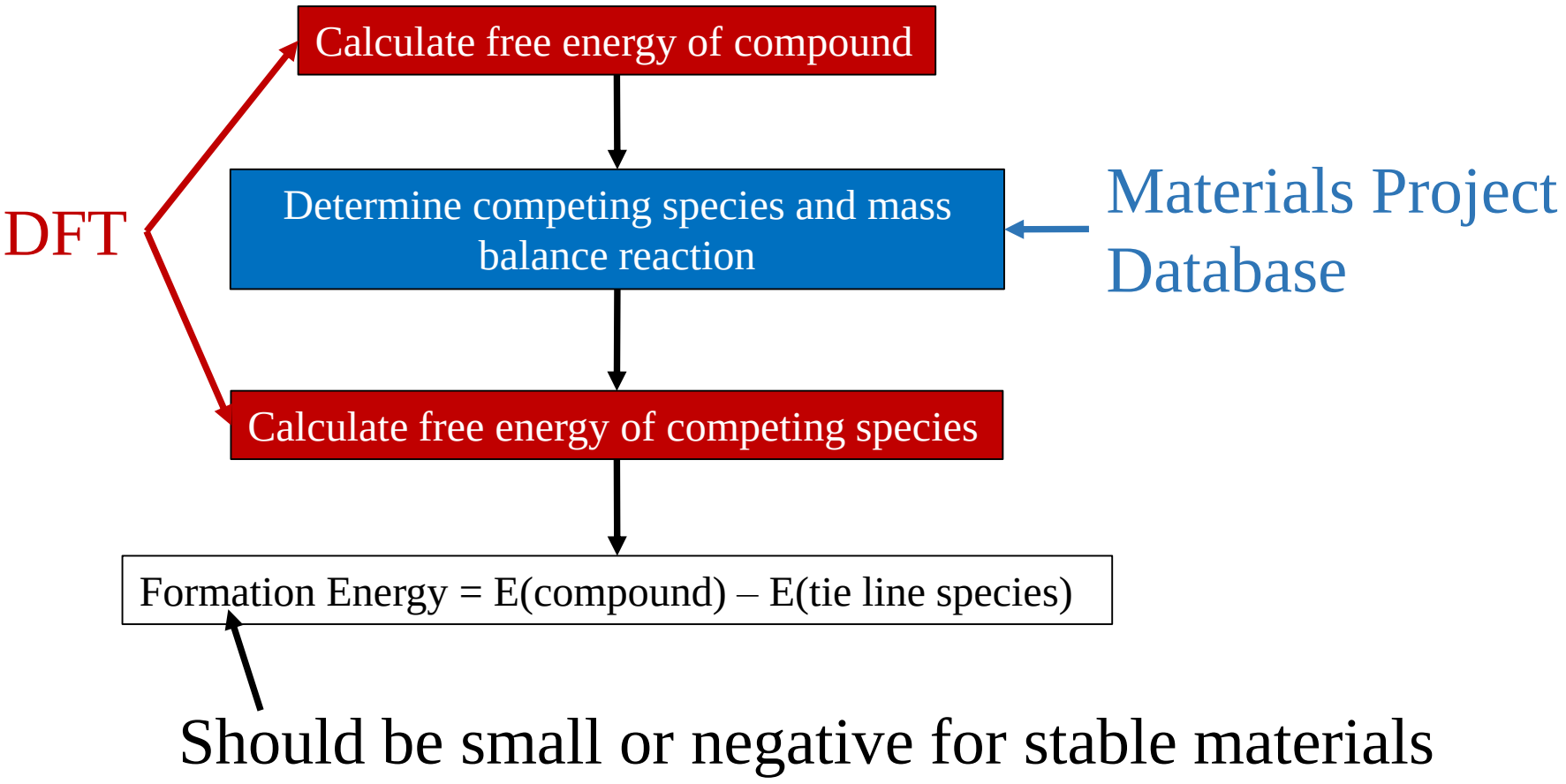

Jain, *et al.*, APL Materials, 2013

Thermodynamic stability of *existing* M_2AX phases

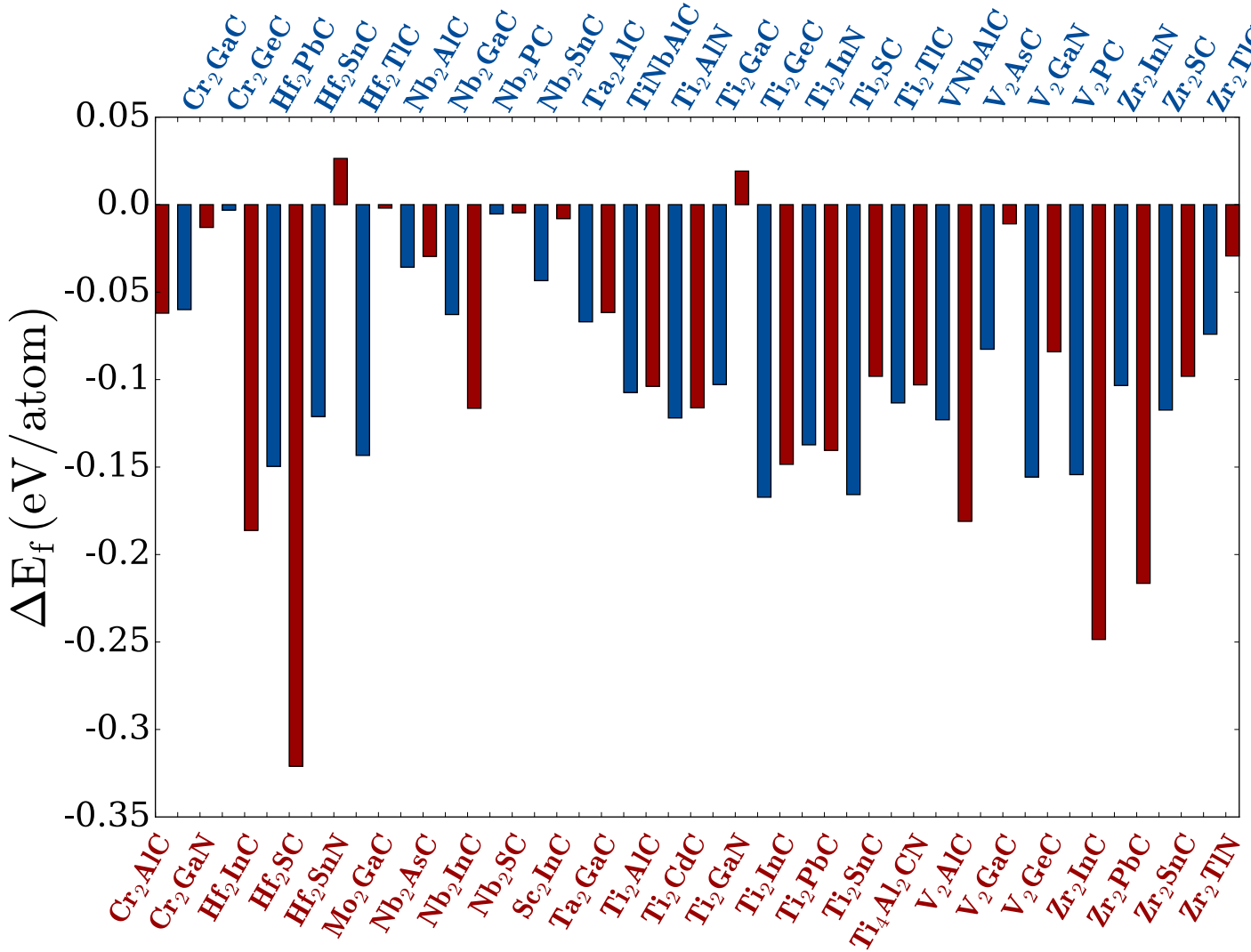

Ashton, *et al.*, Phys. Rev. B (2016)

Stability trends among M_2AX phases

M_2AX

We observe the same “popular” elements in our screening as are present in experimentally synthesized M_2AX phases, only more of them.

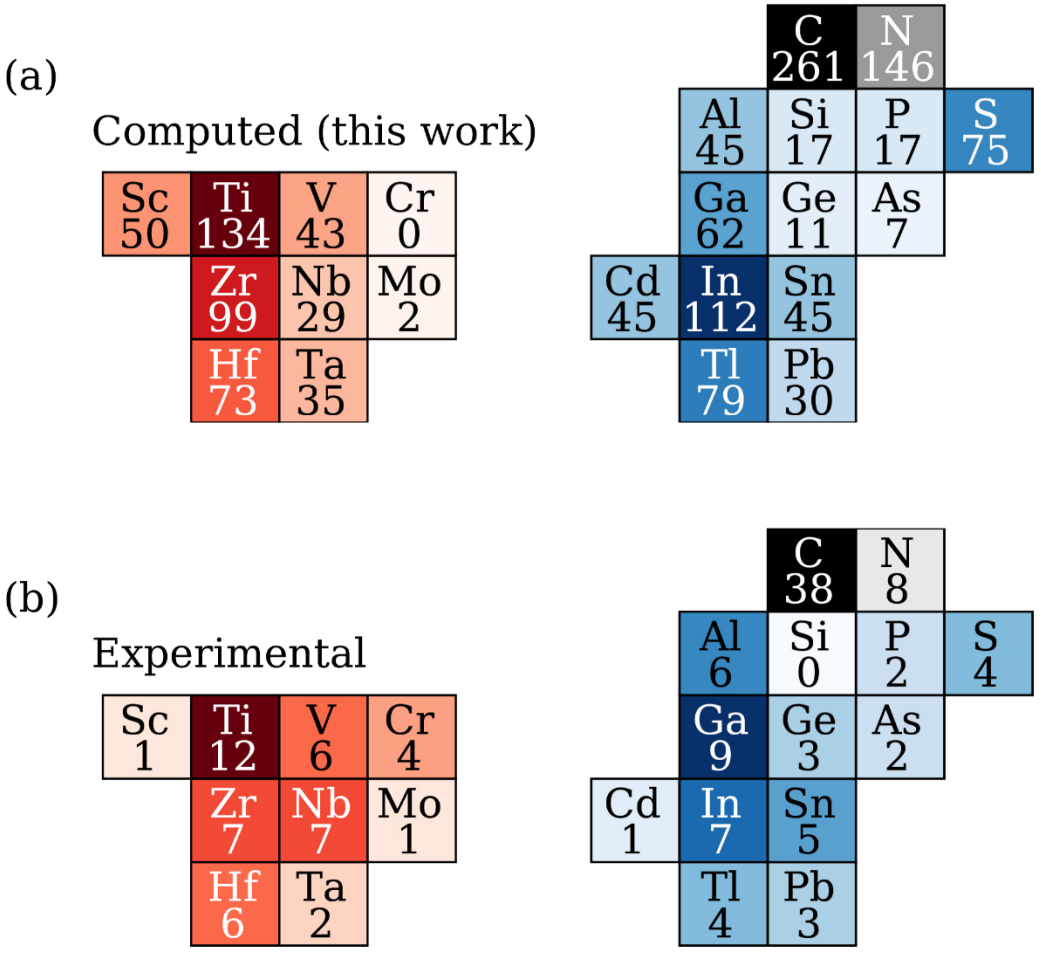

Ashton, *et al.*, Phys. Rev. B (2016)

Stability trends among M_2AX phases

% of M_2AX phases that are stable vs…

Valence mismatch

Radius mismatch

Electronegativity mismatch

Total ionicity

Total # of valence electrons

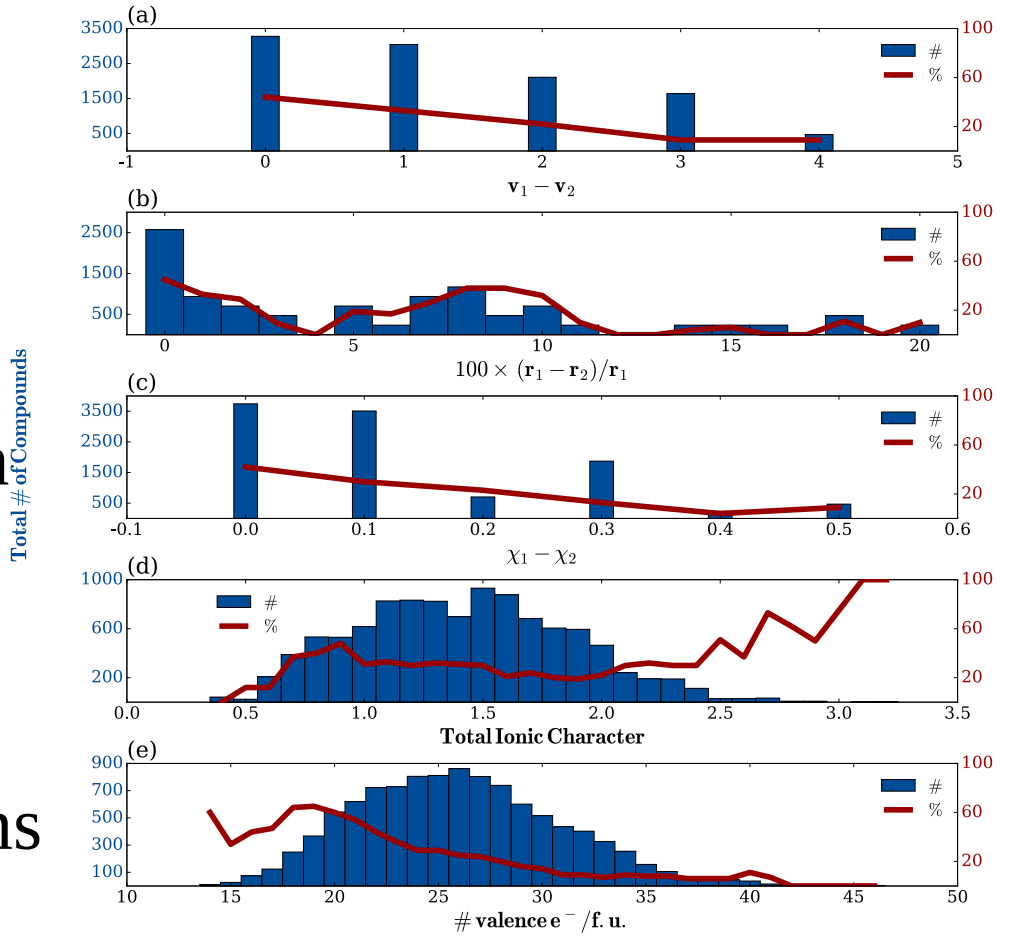

Ashton, *et al.*, Phys. Rev. B (2016)

Magnetic M_2AX phases

Cr_2InN & $Cr_4(CdIn)N_2$ show ferromagnetic ordering at 0K

	Cr_2InN	**$Cr_4(CdIn)N$**
Formation energy (meV/atom)	7	21
Magnetization energy (meV/Cr atom)	68	70
Final magnetic moment (μ_B/Cr atom)	1.08	1.18

Ashton, *et al.*, Phys. Rev. B (2016)

MAX Phase stability

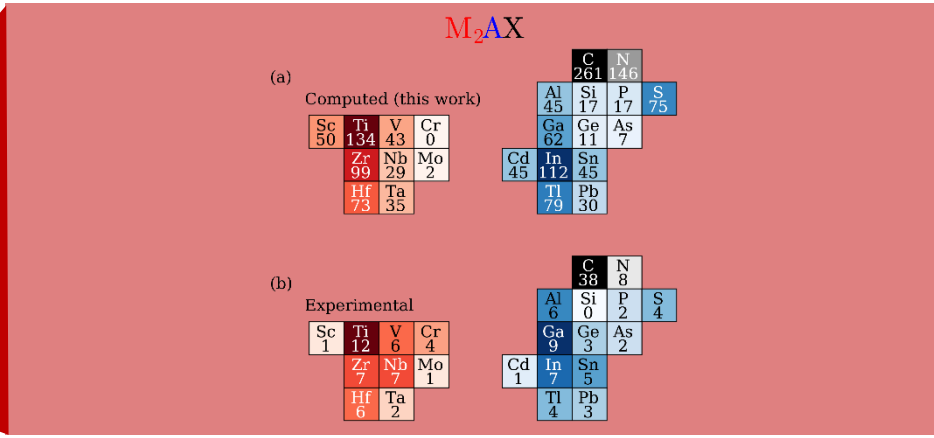

MXene stability

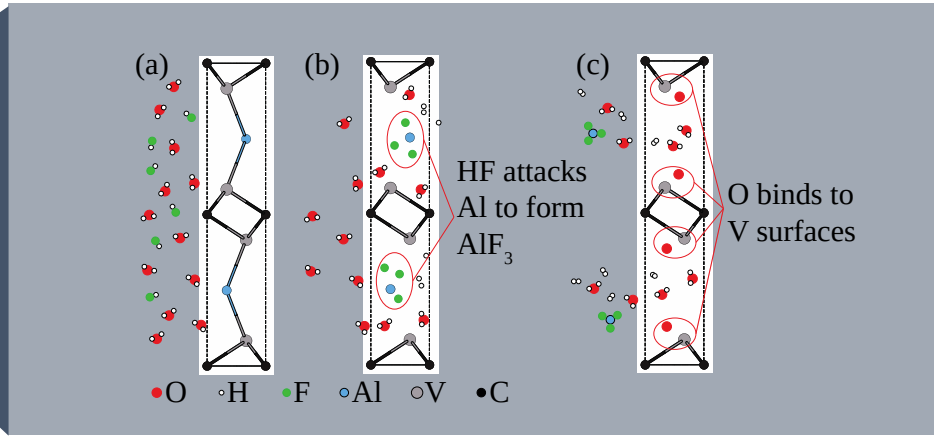

MXenes as LIB anodes

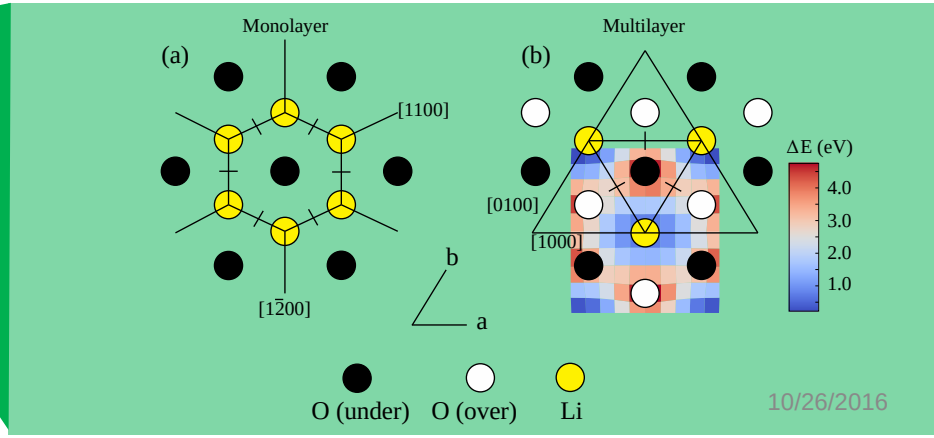

10/26/2016

MXene synthesis

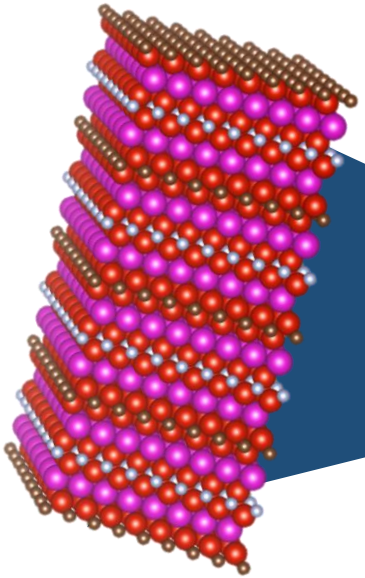

Immersion in H_2O/HF (0.5M)

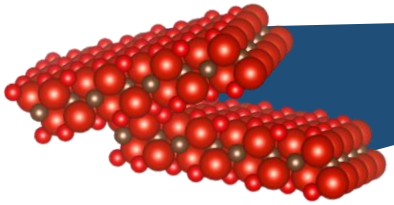

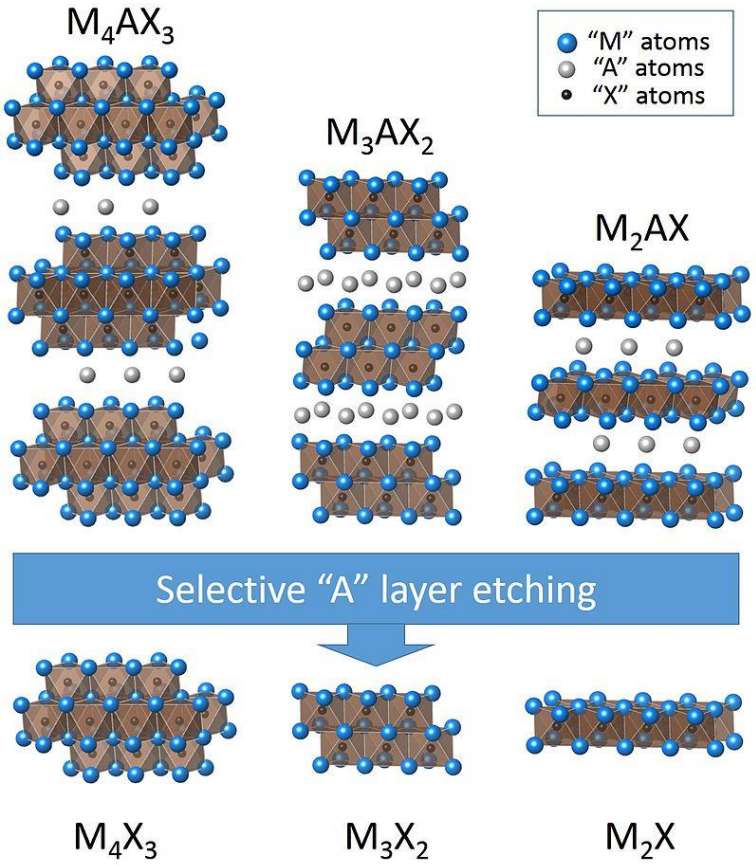

MXene composition

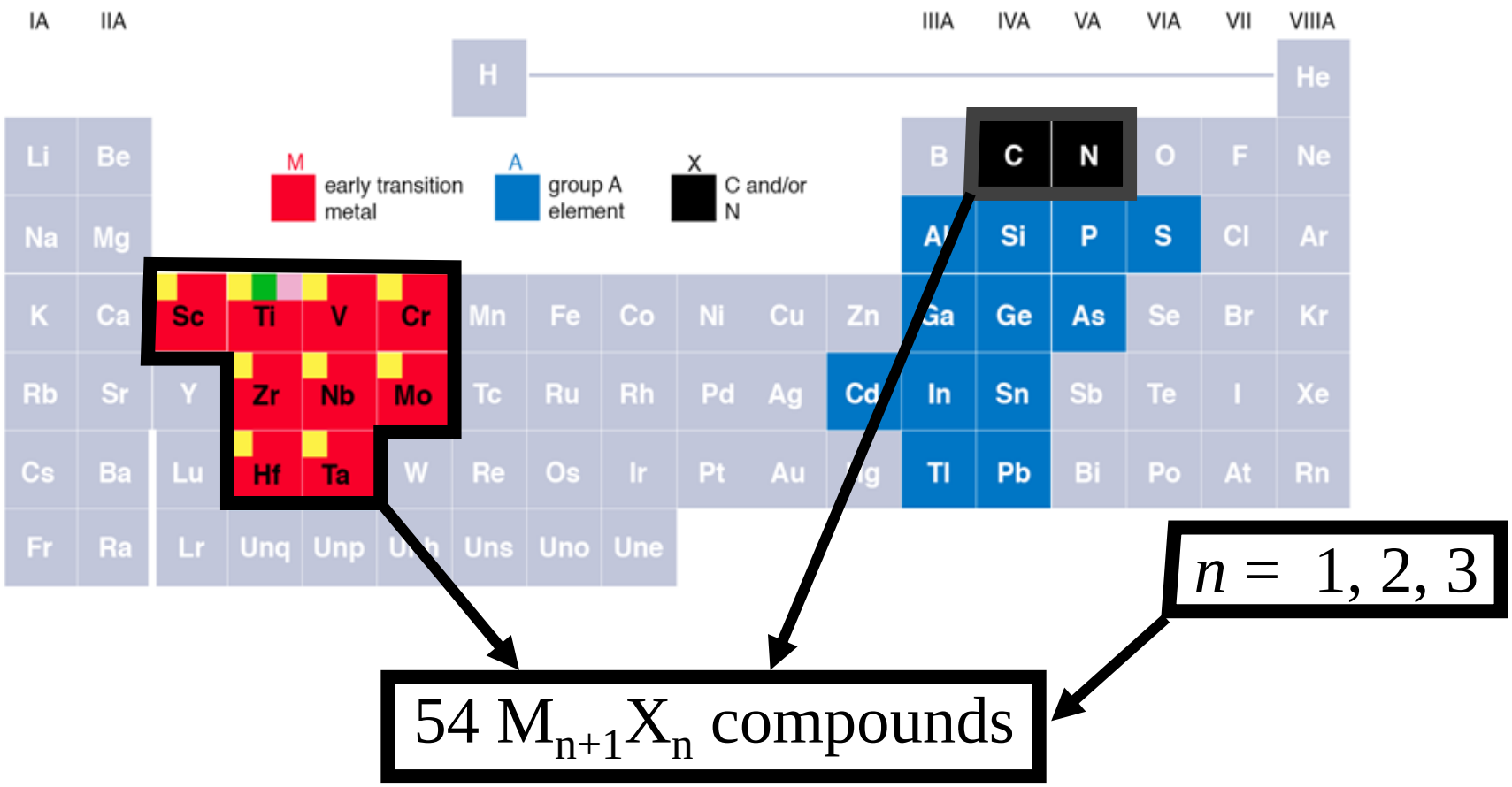

Possible applications for MXenes

- Thermoelectrics
- Sensors
- Catalysts
- Conductive polymer additives
- Solid lubricants
- Li-ion battery anodes

etc.

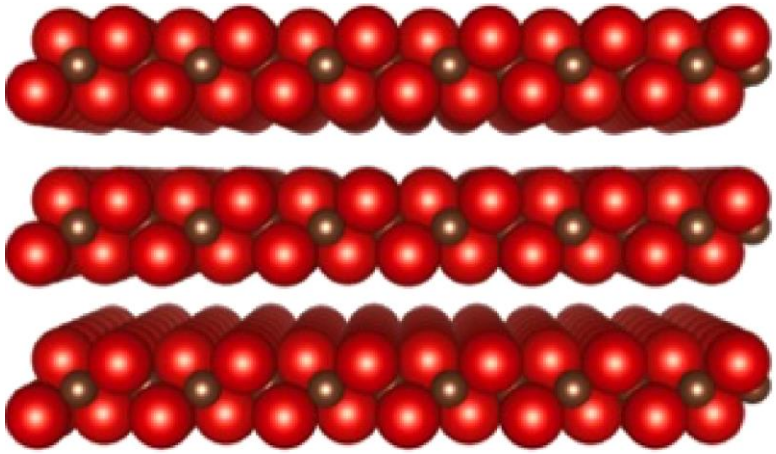

Khazaei, *et al.*, Phys. Chem. Chem. Phys. (2014)
Lukatskaya, *et al.*, Science (2013)
Naguib, *et al.*, Adv. Mater. (2014)

MXenes as dispersion-bound solids

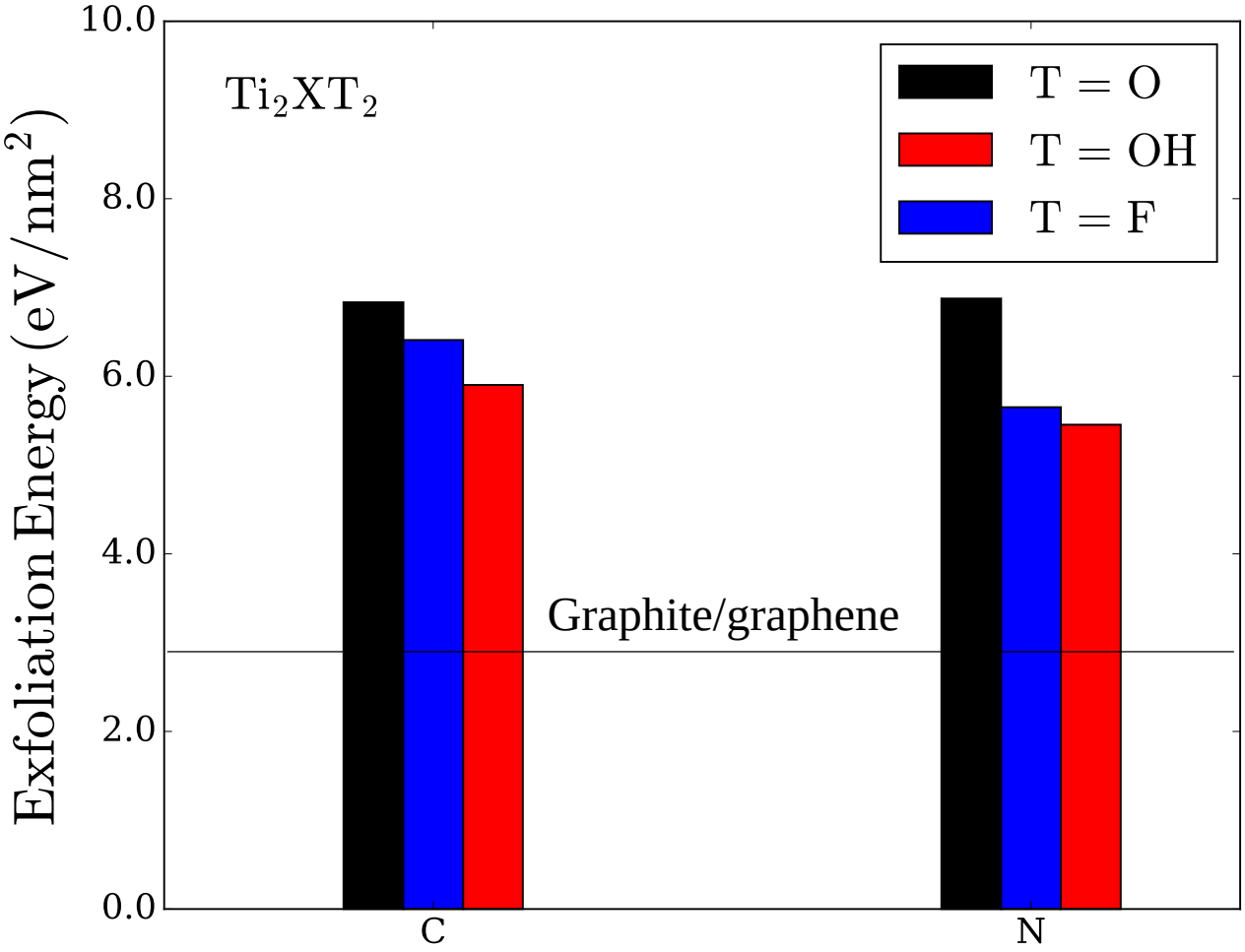

M. Ashton, *et al.*, J. Phys. Chem. C (2016)

MXenes as dispersion-bound solids

$$Ti_2C + 2H_2O \rightarrow Ti_2C\mathbf{O}_2 + 2H_2\ (?)$$

$$Ti_2C + 2H_2O \rightarrow Ti_2C(\mathbf{OH})_2 + H_2\ (?)$$

$$Ti_2C + 2HF \rightarrow Ti_2C\mathbf{F}_2 + H_2\ (?)$$

Because of their high surface area/volume ratio, the species on MXene surfaces are a significant part of the overall stoichiometry.

Ashton, *et* al., J. Phys. Chem. C (2016)

MXene surface saturation

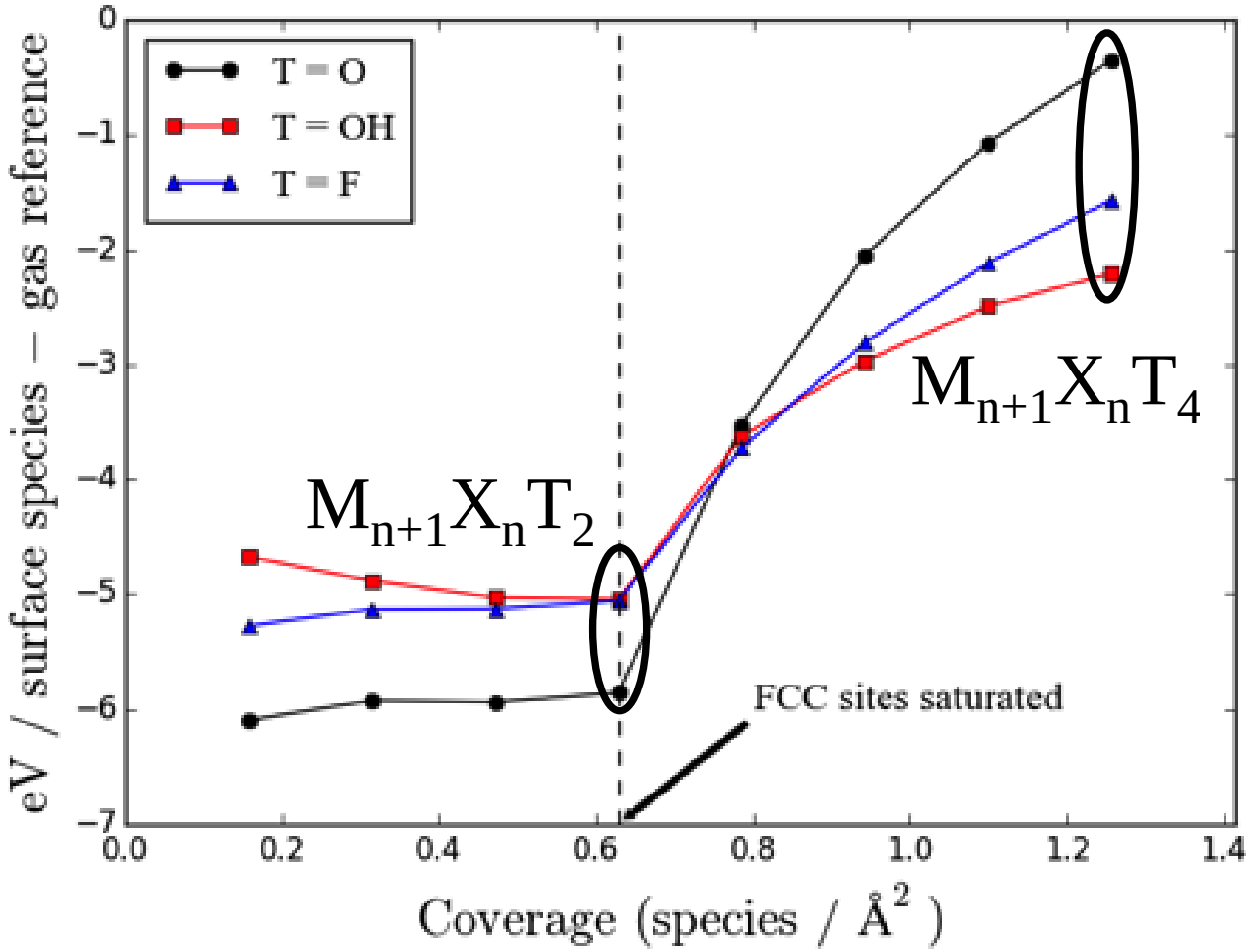

Ashton, *et al.*, J. Phys. Chem. C (2016)

Comparing O, F, & OH binding energies

$$E_b = E(M_{n+1}X_nT_m) - E(M_{n+1}X_n) - \frac{m}{2}E(T_2) - m\mu_T$$

Coated MXene

Bare MXene

Surface species reference

Surface species chemical potential

All depend on $\boldsymbol{\mu_H}$

$$\mu_O = \Delta G_f^{H_2O} - 2\boldsymbol{\mu_H}$$

$$\mu_{OH} = \Delta G_f^{H_2O} - \boldsymbol{\mu_H}$$

$$\mu_F = \Delta G_f^{HF} - \boldsymbol{\mu_H}$$

Ashton, *et al.*, J. Phys. Chem. C (2016)

Comparing O, F, & OH binding energies

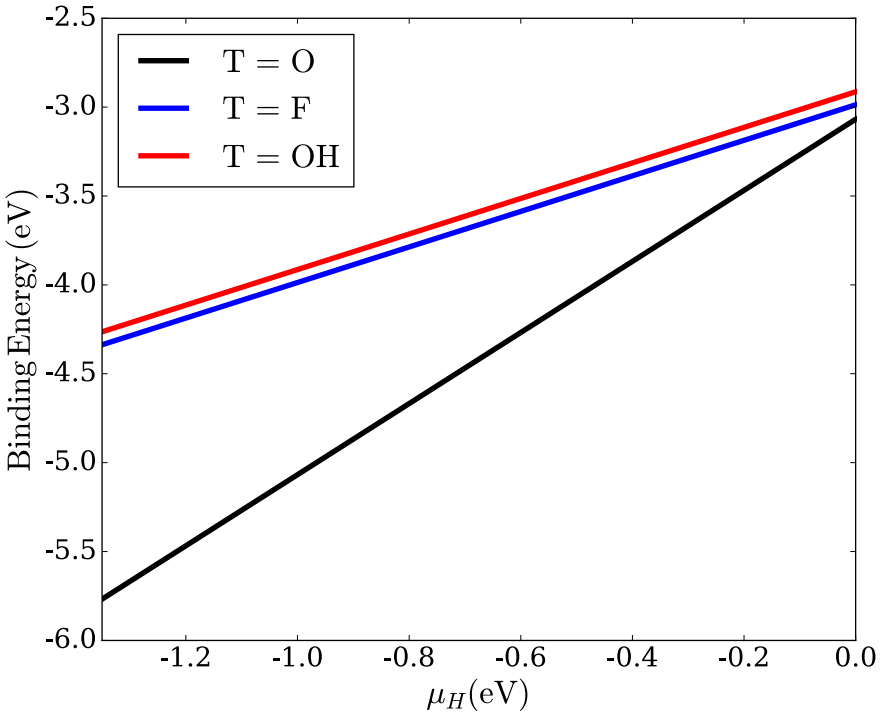

Ti_2C

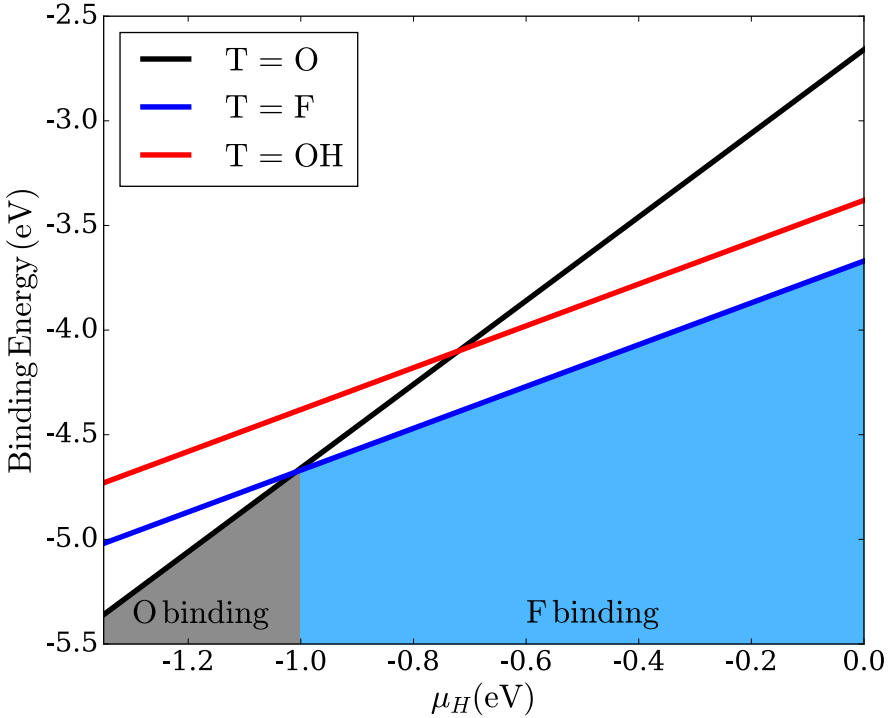

Sc_2C

For all transition metals other than Sc, O binding is preferred for all μ_H.

Ashton, *et al.*, J. Phys. Chem. C (2016)

Example etching reaction: V_2AlC/V_2CO_2

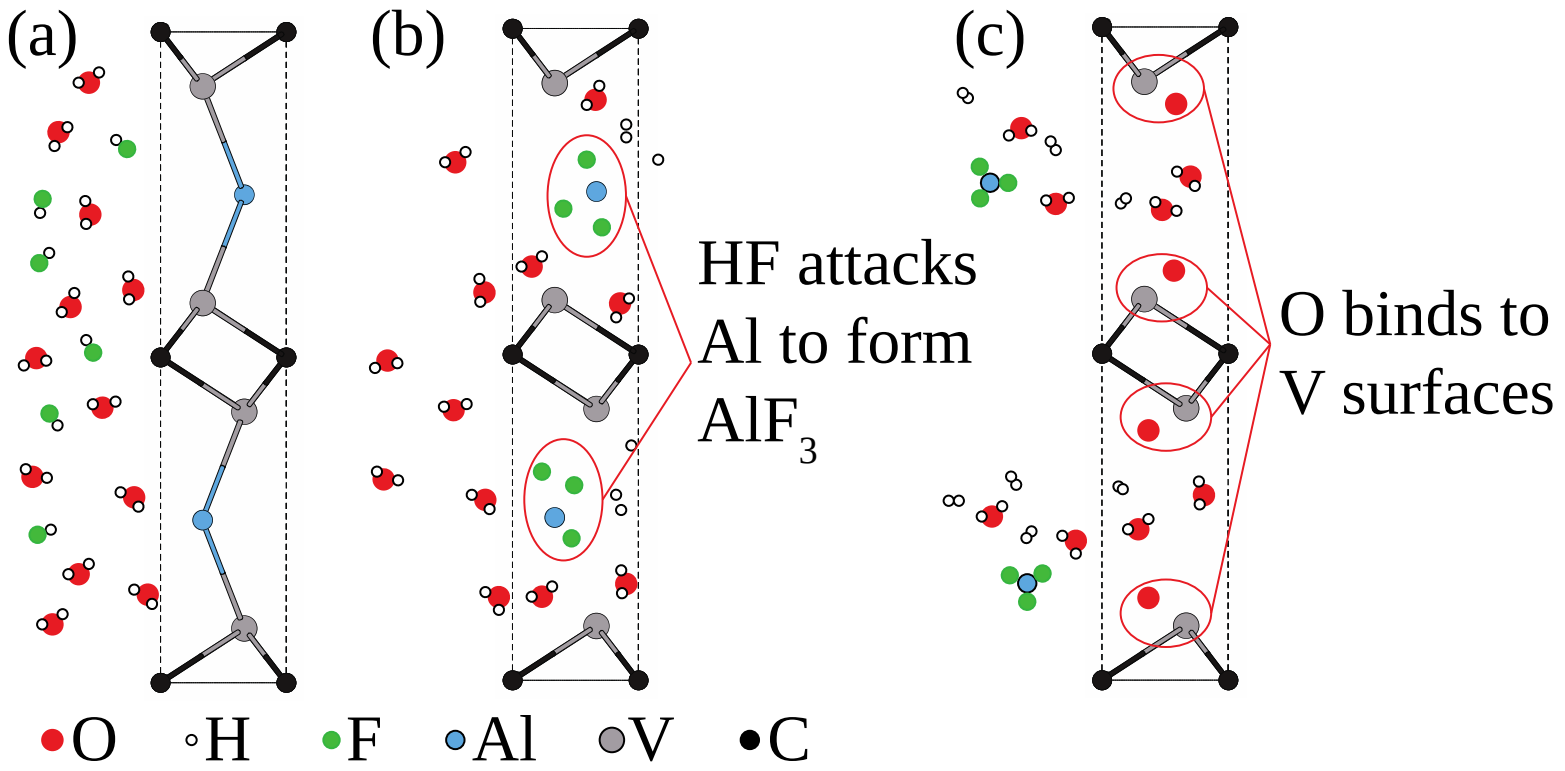

2D material formation energies

Example: $E_f(Ti_2CO_2) = E(Ti_2CO_2) - E(TiC) - E(TiO_2)$

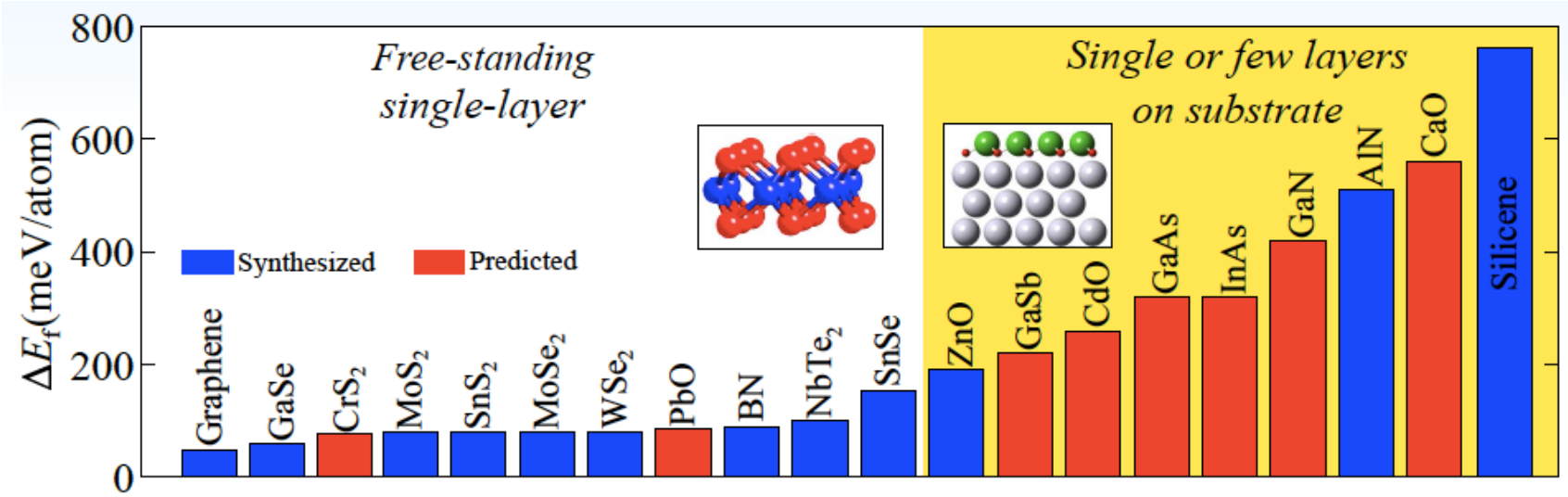

2D materials will never be "stable" compared to 3D competing phases, but with a low enough metastability they can be stabilized kinetically.

MXene formation energies

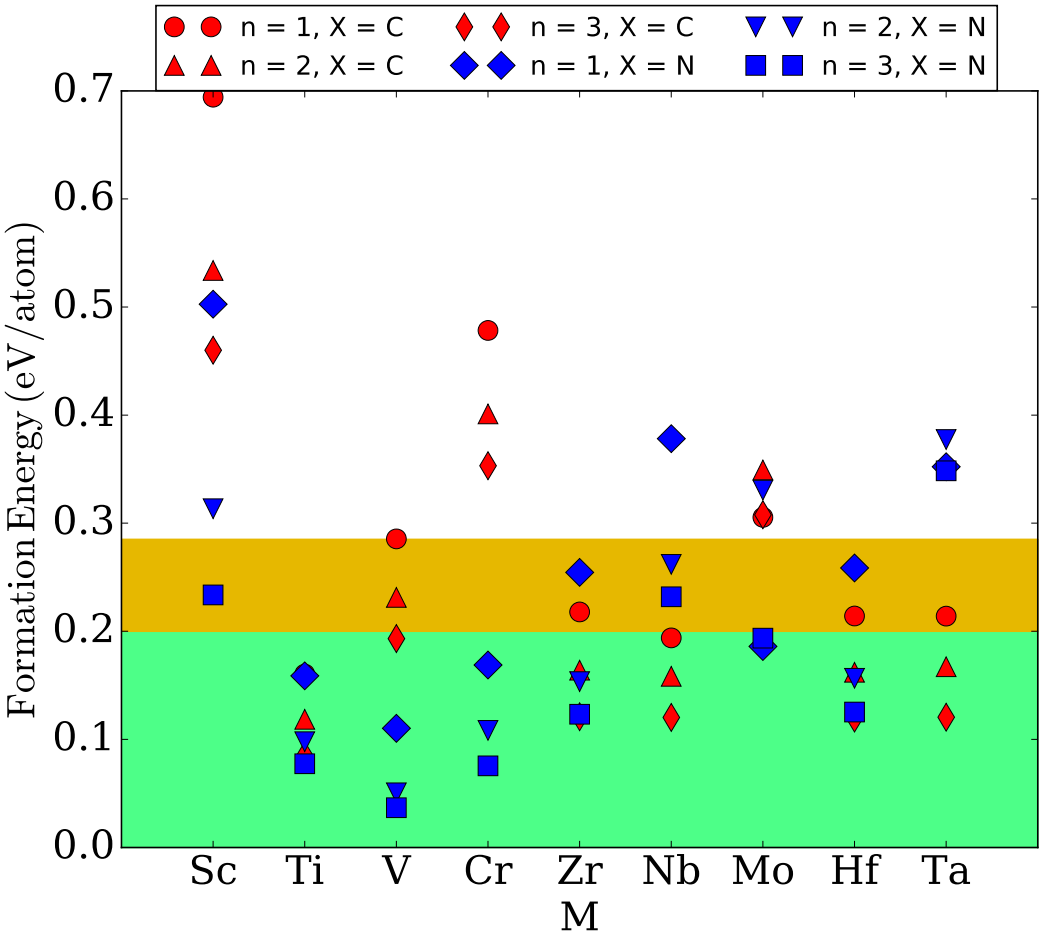

V_2CO_2 has the highest formation energy of all MXenes that have been synthesized to date.

All MXenes below V_2CO_2 (within the yellow threshold) should be creatable from a thermodynamic perspective.

Ashton, *et al.*, J. Phys. Chem. C (2016)

MAX Phase stability

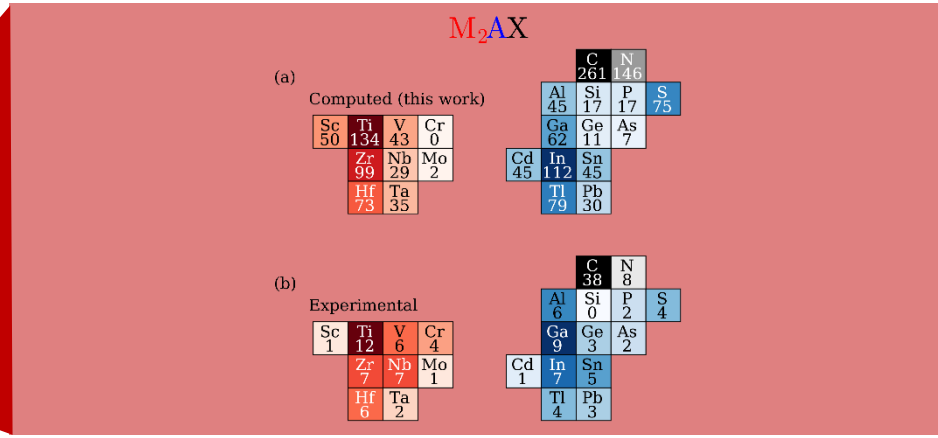

MXene stability

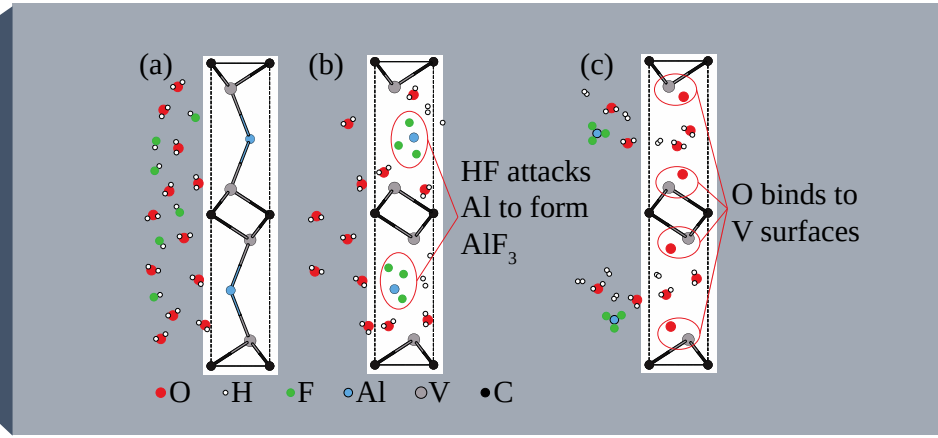

MXenes as LIB anodes

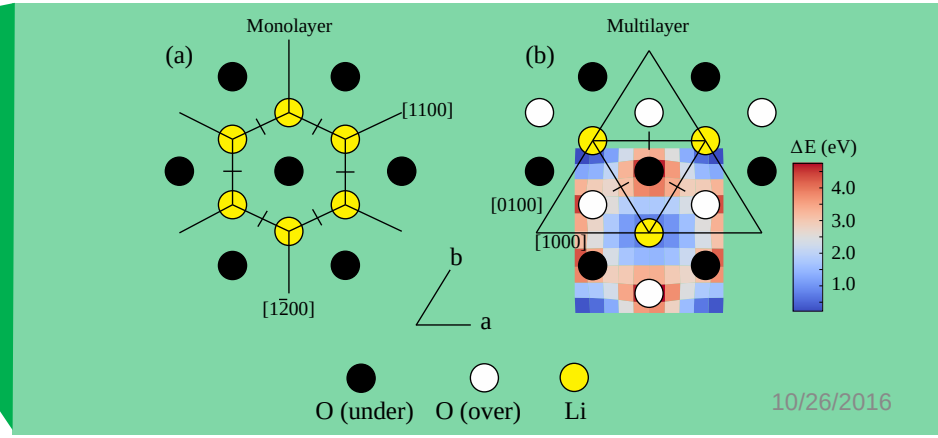

10/26/2016

Li-Ion battery anode candidate criteria

- Stable ✓
- Lightweight ✓
- Inexpensive ✓
- High capacity
- Low diffusion barrier
- Minimal swelling during charge/discharge

} $Ti_{n+1}C_nO_2$ & $V_{n+1}C_nO_2$

MXenes as Li-ion battery anodes: The competition

	Si	Graphite
Li storage capacity ($mAhg^{-1}$)	3579	372
Li diffusion barrier (eV)	0.5	0.3-1.5
Lithiation volume change (%)	280	10
Conductive	No	Yes

Tang, et. al., J. Am. Chem. Soc. 134, 16914 (2012)
Lukatskaya, et. al., Science 341, 1502 (2013)
Wang et al., Nano Lett. 13, 5578−5584 (2013)
Tritsaris et al., *J. Phys. Chem. C 116* (42), 22212–22216 (2012)
T. Kawai, Japanese Journal of Applied Physics 52 04CN08 (2013)
M. Patterson, http://nano.indiana.edu/documents/MPatterson.pdf

Diffusion pathways in multilayer MXenes

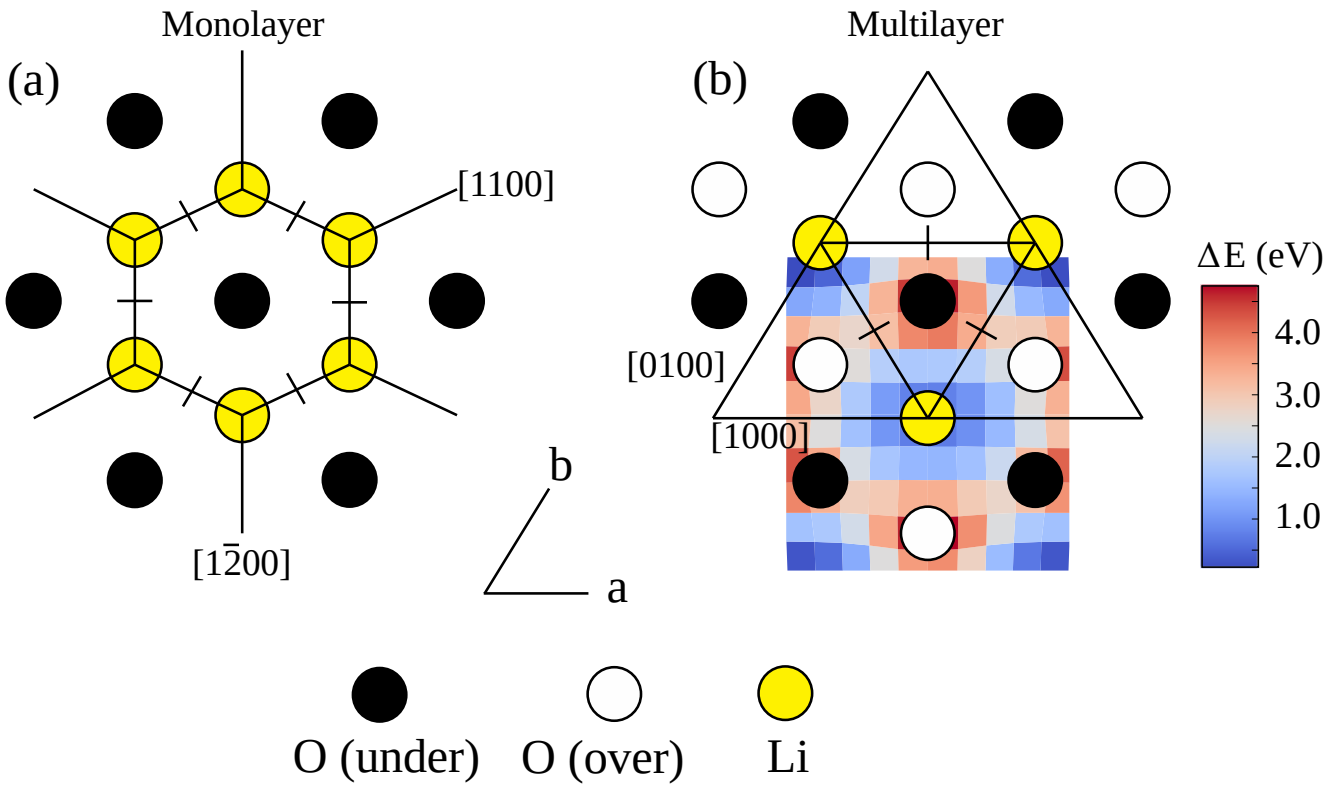

Ashton, *et al.*, Appl. Phys. Lett. (2016)

Voltage profiles

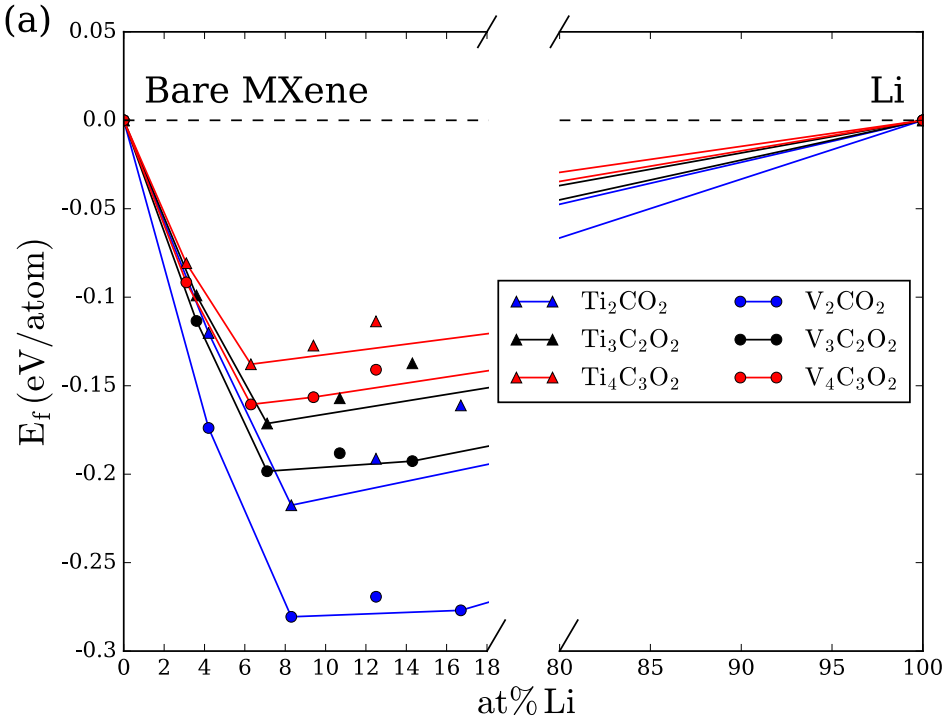

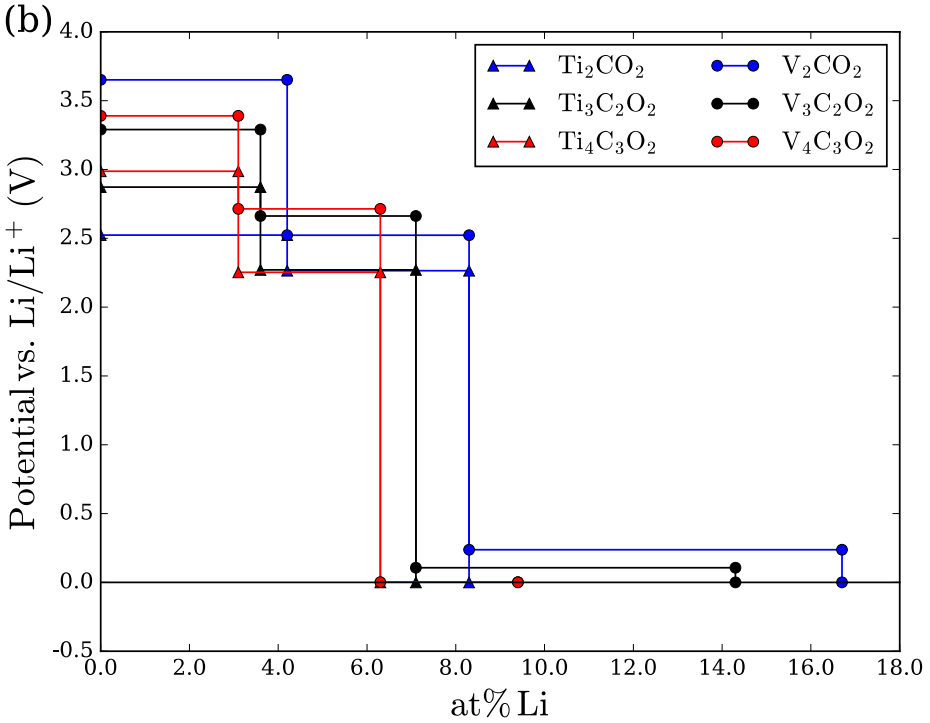

$$V = -\frac{E\left(M_{n+1}X_nO_2Li_{x_1}\right) - E\left(M_{n+1}X_nO_2Li_{x_0}\right) - (x_1 - x_0)E(Li)}{x_1 - x_0}$$

Ashton, *et al.* Appl. Phys. Lett. (2016)

Comparison of anode-related properties

MXene	Gravimetric Capacity (mAh/g)	Volumetric Capacity (Ah/L)	Volume Expansion (%)	Diffusion Barrier (eV)
Ti_2CO_2	192	346	0.32	0.63
$Ti_3C_2O_2$	134	240	-0.1	0.60
$Ti_4C_3O_2$	103	187	0.34	0.73
V_2CO_2	276	379	2.82	0.82
V_3CO_2	192	263	1.93	0.52
$V_4C_3O_2$	148	205	1.64	0.42

Ashton, *et al.*, Appl. Phys. Lett. (2016)

Summary of MAX and MXene findings

- 10,530 MAX phase precursors screened for stability
  - 301 have formation energies < -100 meV/atom
  - Cr_2InN and Cr_4CdInN_2 appear to be ferromagnetic with appreciable moments

- 54 MXenes screened for stability
  - 38 fall within the 285 meV/atom threshold of MXene stability

- 6 MXenes investigated as LIB anodes
  - V_2CO_2 showed most promise as a high-capacity anode
  - $V_4C_3O_2$ showed most promise as a high-power anode

Water Interactions with Metal Surfaces

Andrew Antony, Tao Liang, Michael Janik, and Susan B. Sinnott
Department of Materials Science and Engineering
Penn State University
University of Florida

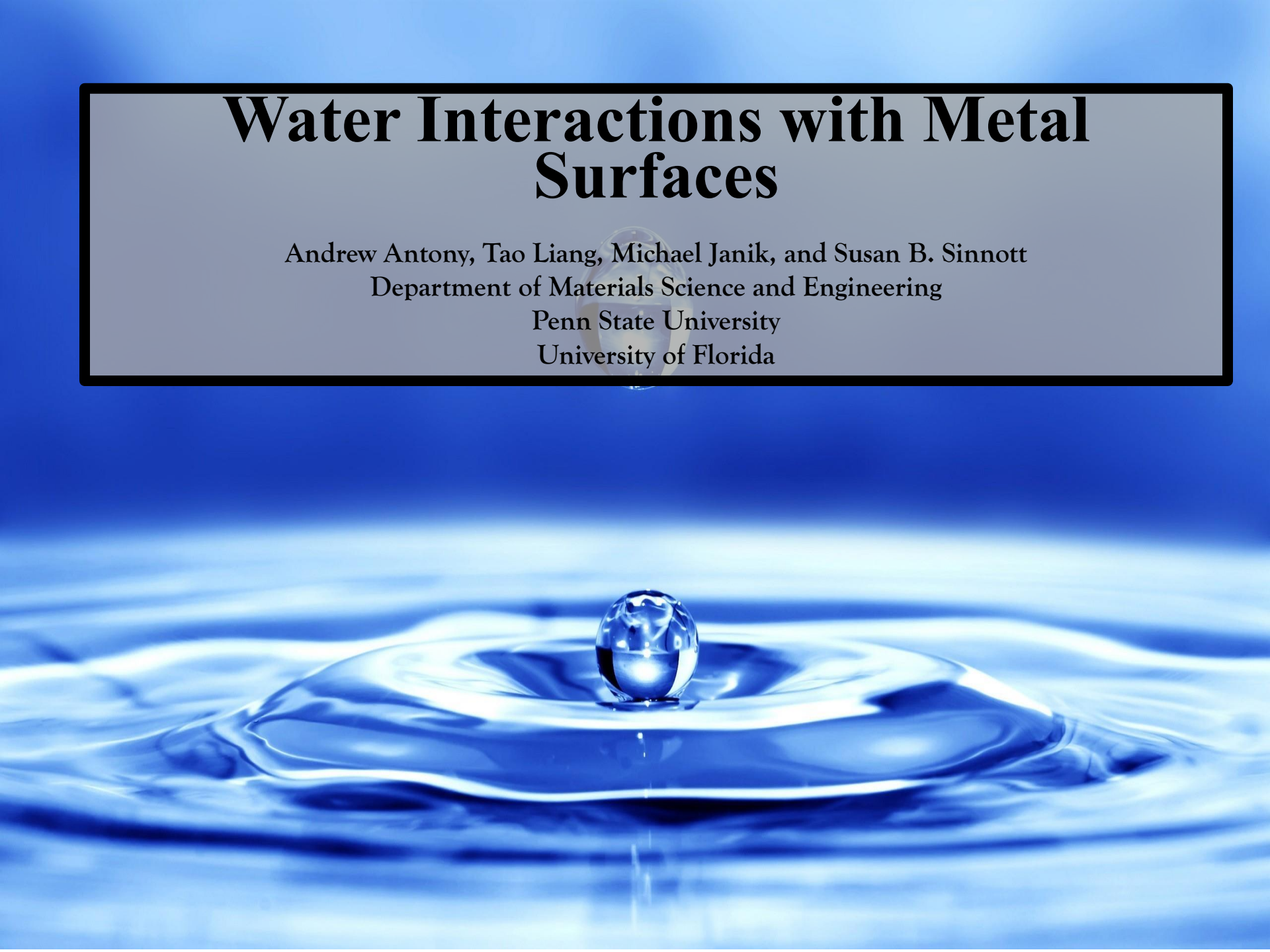

Properties of 3rd Generation Charge Optimized Many-Body (COMB3) Potential

Properties	TIP3P	TIP4P	SPC	SPC/E	Exp./DFT	COMB3
H_2O molecule						
Charge on O, q_o (e)	-0.83	-1.04	-0.82	-0.82	-	-0.71
Dipole moment (eÅ)	0.50	0.62	0.49	0.49	0.39	0.42
Ice_Ih						
Charge on O, q_o (e)	-0.83	-1.04	-0.82	-0.82	-	-0.87
Dipole moment (eÅ)	0.50	0.62	0.49	0.49	0.52[g], 0.64[h]	0.53
Liquid H_2O						
$\Delta H_f (eV/H_2O)$					-2.96	-2.81
density (g/cm^3)	0.99	0.99	0.98	1.00	1.00	1.00
Average water dipole moment (eÅ)	0.49	0.45	0.47	0.49	0.60	0.45
Diffusion coefficient (10^{-5} cm^2/s)	5.30	3.90	4.02	2.52	2.30	0.96

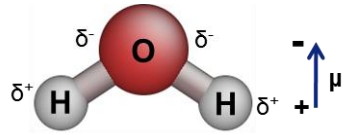

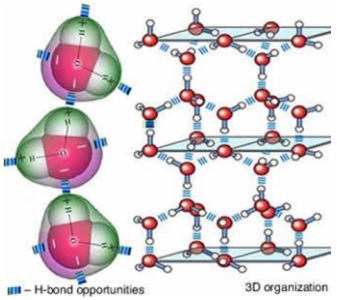

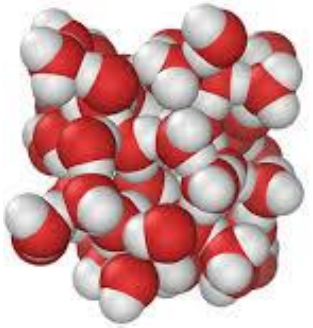

Antony, *et al.*, Langmuir (2016)

PennState

Functional Form of the COMB3 Potential

$$E_T = \sum_i \left\{ E_i^{Self}(q_i) + \frac{1}{2}\sum_{j\neq i}\left[V_{ij}^{short}(r_{ij}, q_i, q_j) + V_{ij}^{Coul}(r_{ij}, q_i, q_j)\right] + B_i(q_i) + C_i(r_{ij}, \theta_{ijk}) + E^{polar}(q_i, r_{ij}) + E^{vdW}(r_{ij}) \right\}$$

- **Self energy**: ionization energies and electron affinities; includes penalty function to capture change in self-energy due to the field from the ionic lattice
- **Short-range interactions**: reactive bond-order potential
- **Coulomb interactions**: Coulomb integral over the charge densities
- **Charge and angular correction terms**
- **Polarization**: Atomic polarizabililty for organic systems
- **van der Waals energy**

S.R. Phillpot and S.B. Sinnott, Science (2009)
T. Liang et al., Materials Science and Engineering R (2013)

PennState

Predicted RDF of Liquid Water

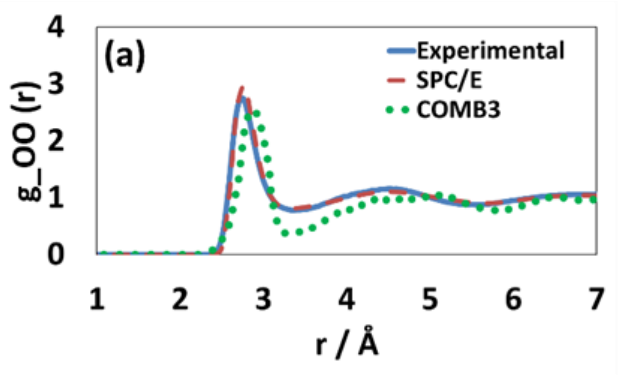

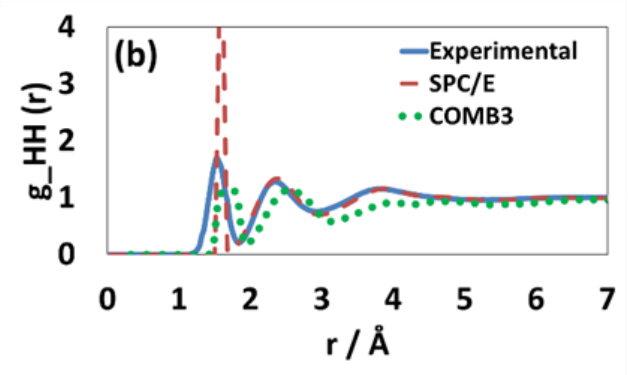

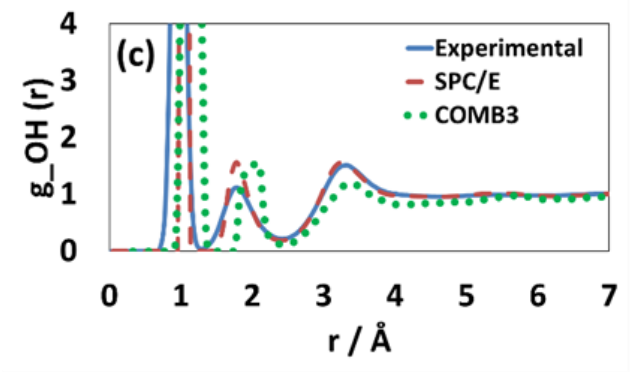

Antony, *et al.*, Langmuir (2016)

PennState

Water Adsorption on Cu (111)

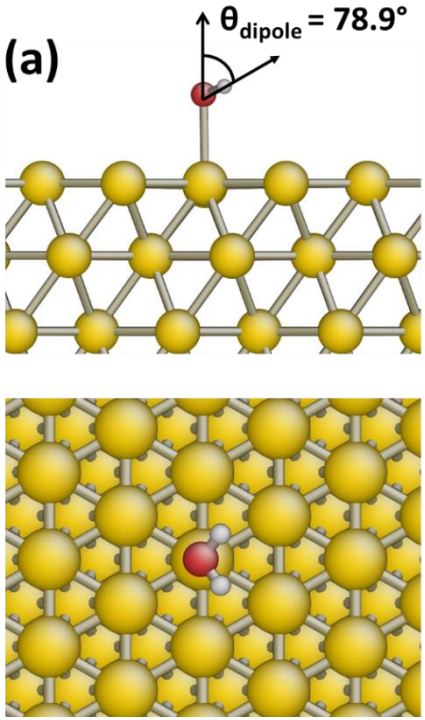

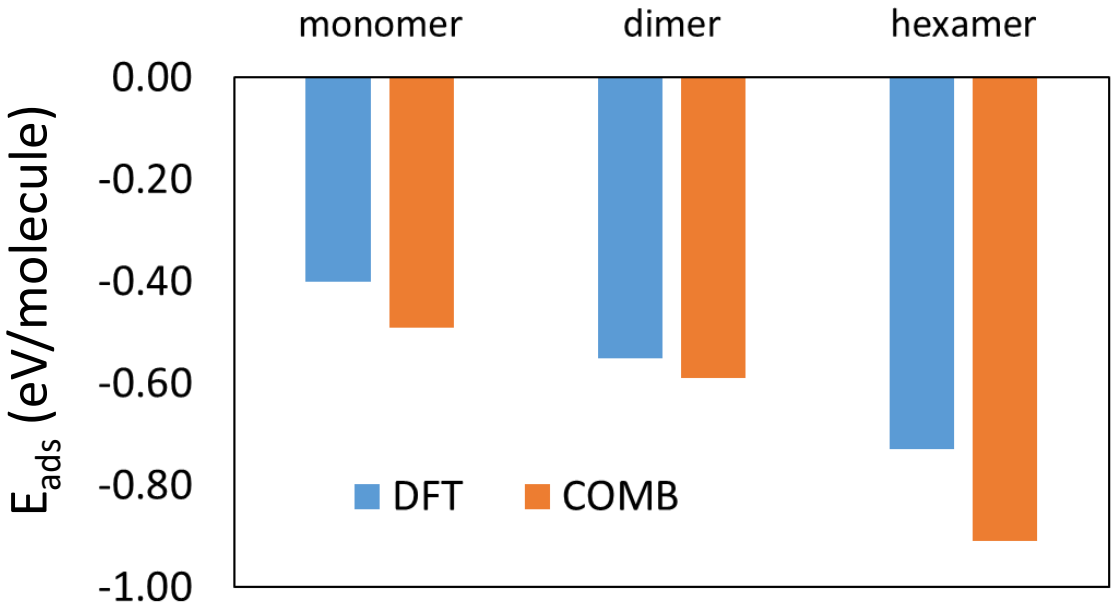

Antony, *et al.*, Langmuir (2016)

PennState

MD simulations of water spreading on bare Cu(111)

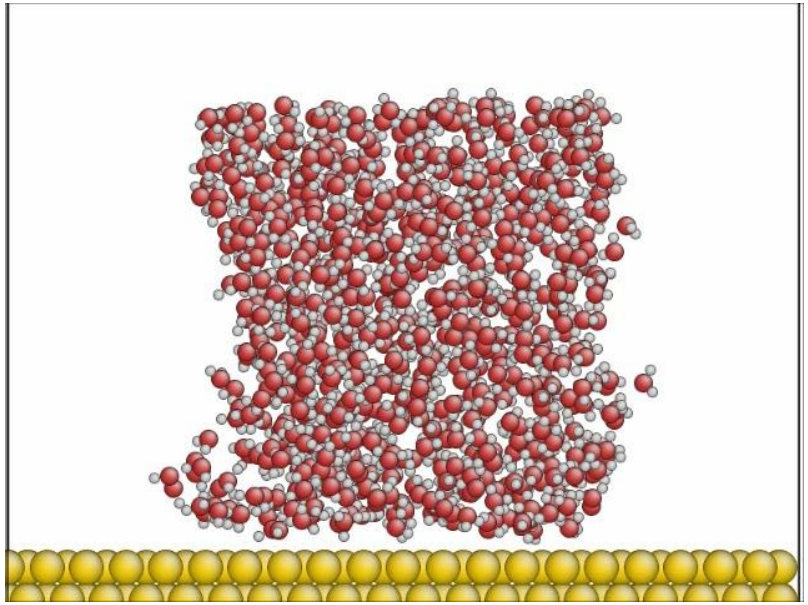

Side view

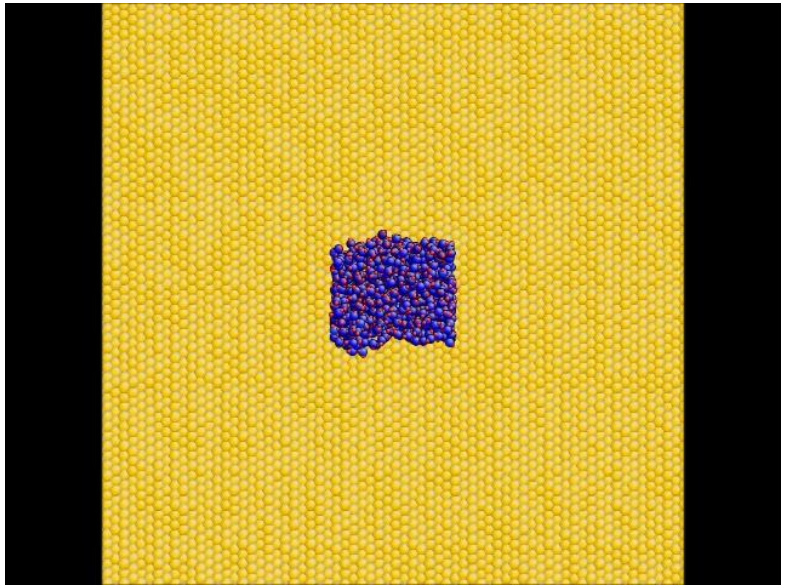

Top-down view
Atoms colored according to charge

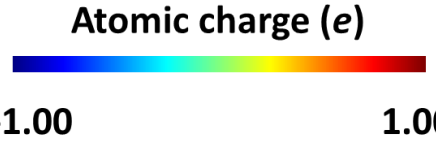

Antony, *et al.*, Langmuir (2016)

PennState

Identified Regions of the Water Droplet

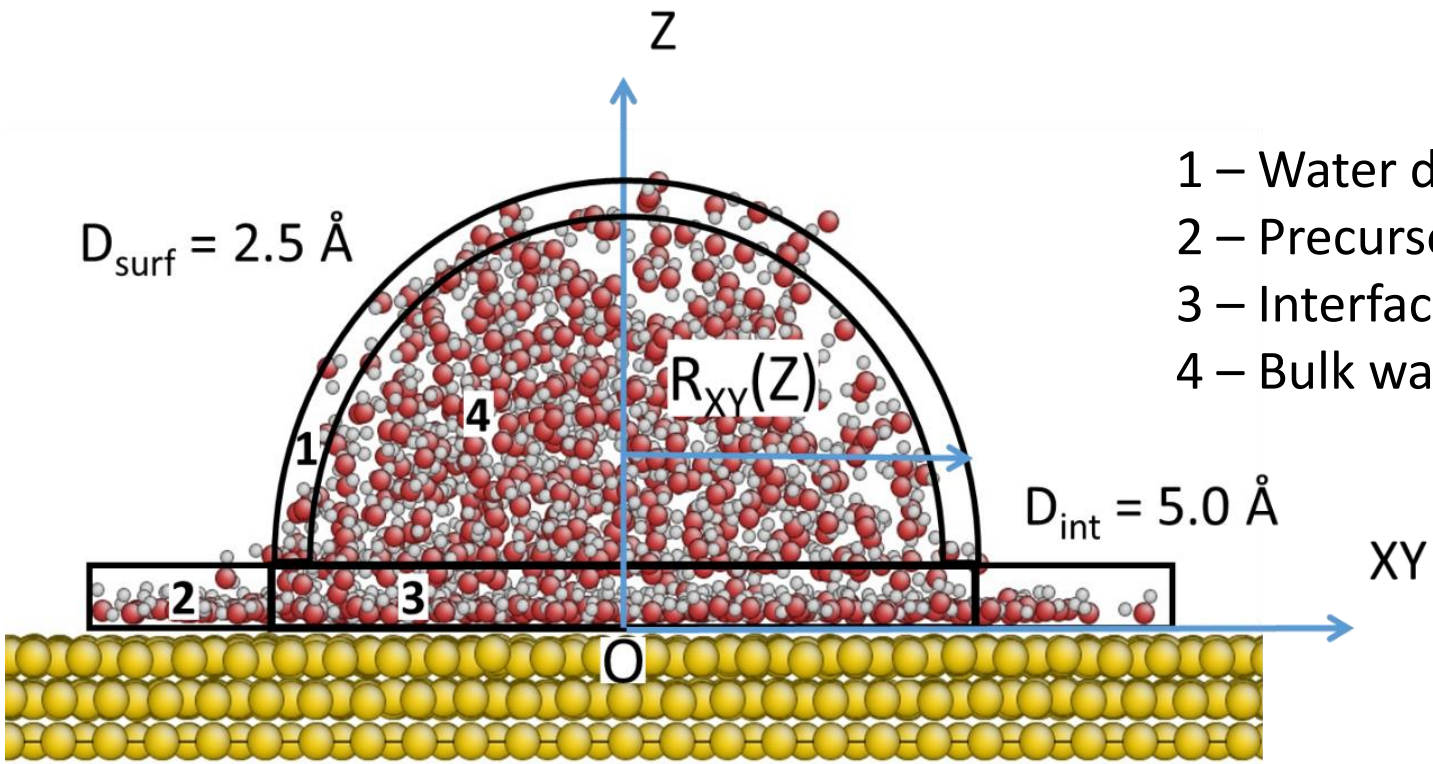

1 – Water droplet surface
2 – Precursor film (PF)
3 – Interfacial water
4 – Bulk water

Antony, *et al.*, Langmuir (2016)

PennState

Propagation of the Droplet Radius

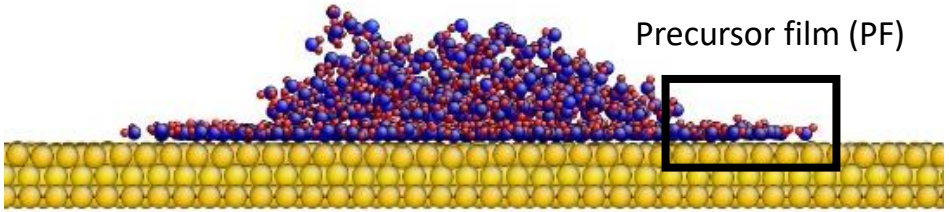

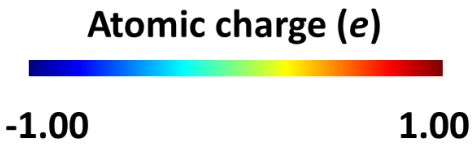

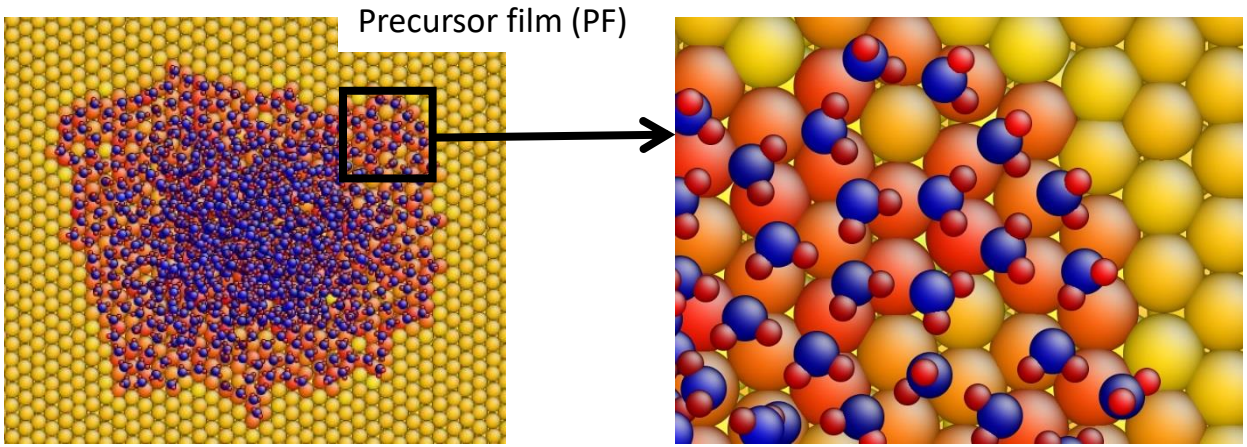

Antony, *et al.*, Langmuir (2016)

PennState

Mean Square Displacement of Wetting

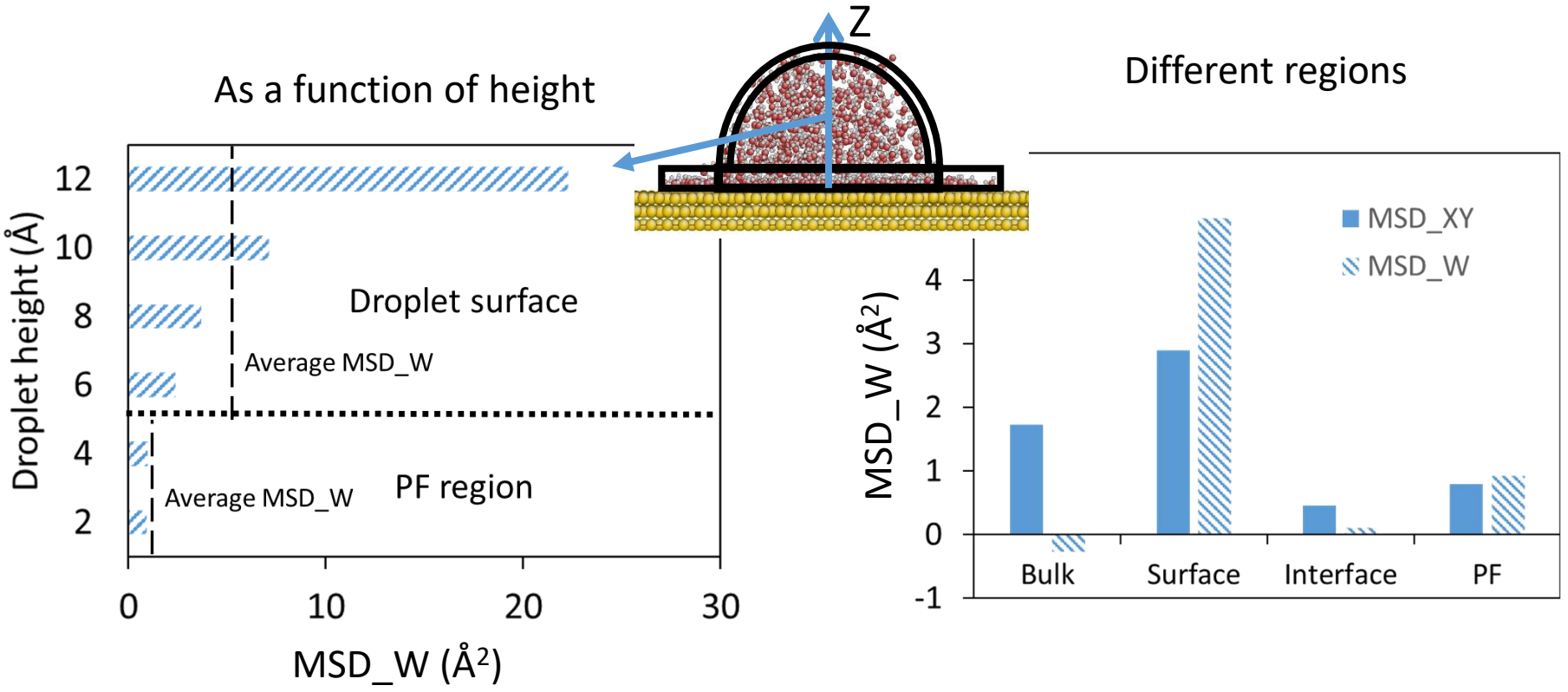

Antony, *et al.*, Langmuir (2016)

PennState

Kinetics of Wetting

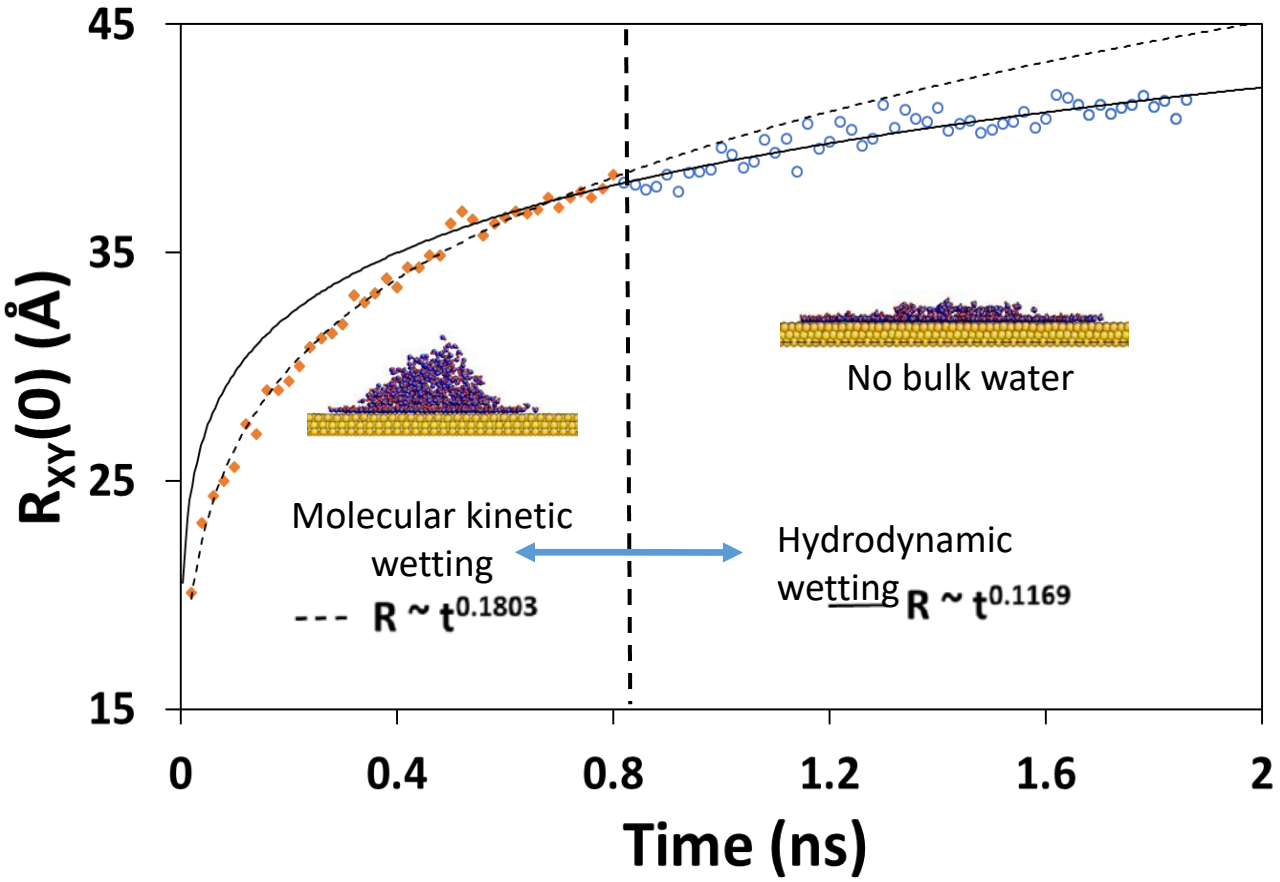

Antony, *et al.*, Langmuir (2016)

PennState

Chemically functionalized Cu(111): O* (left) and OH* (right) covered surfaces

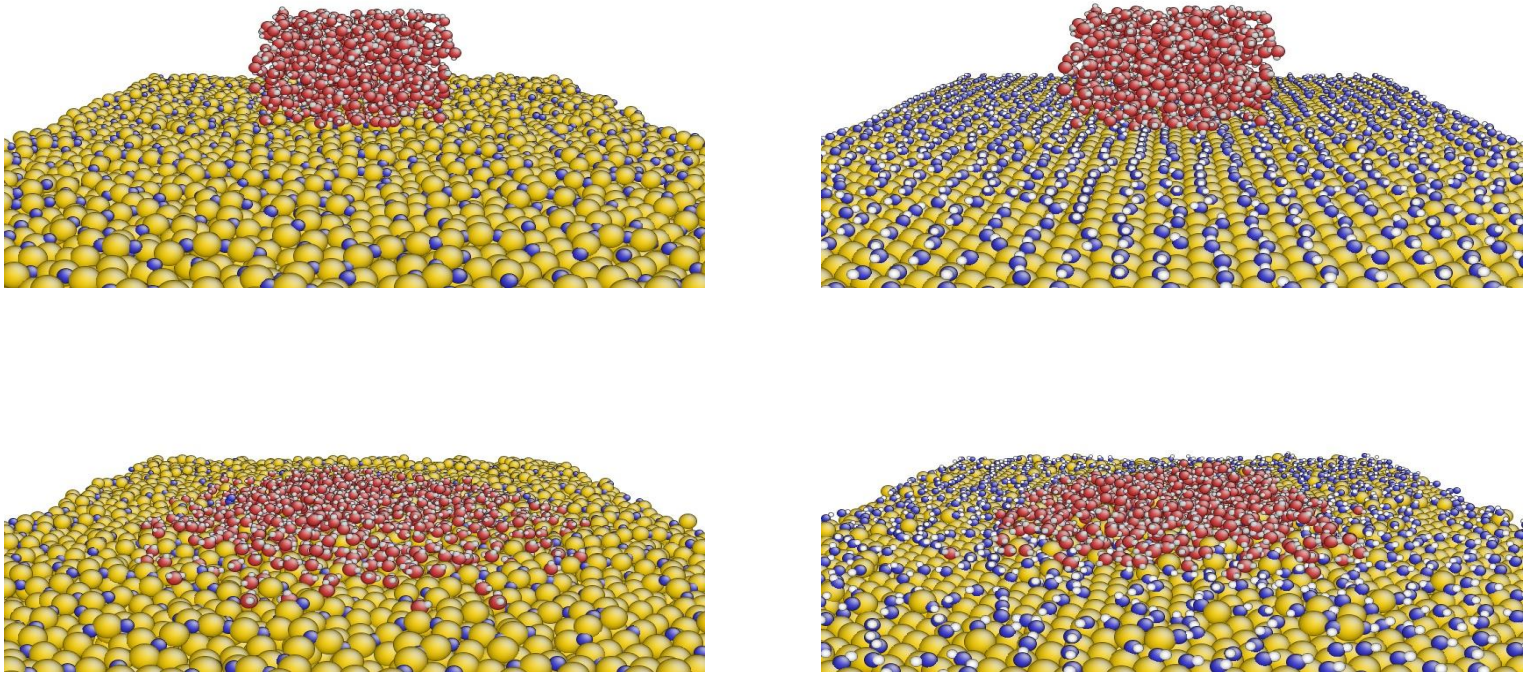

Antony, *et al.*, Langmuir (2016)

PennState

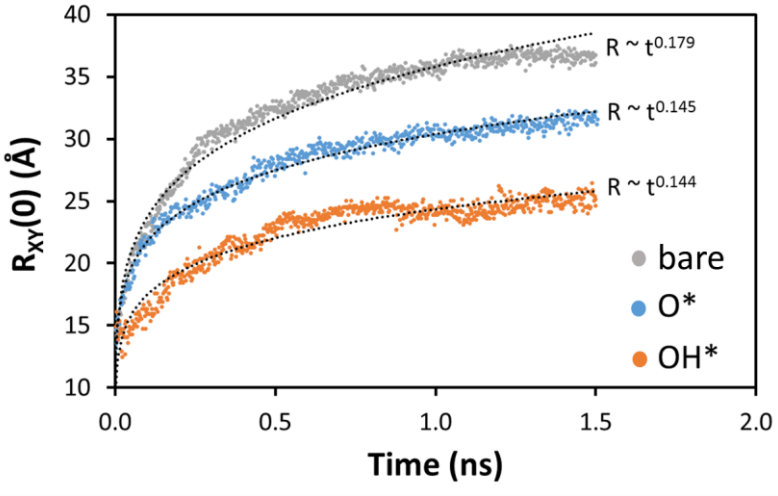

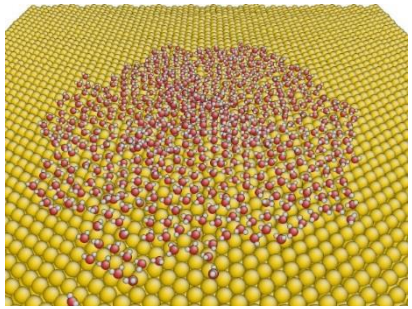

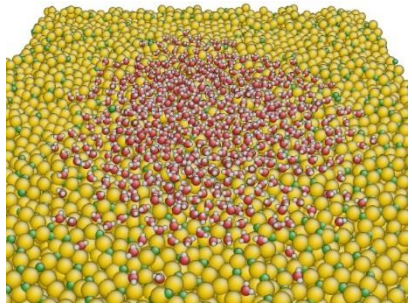

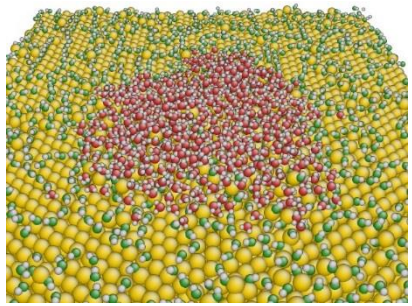

bare Cu(111)

oxidized Cu(111)

hydroxylated Cu(111)

Antony, *et al.*, Langmuir (2016)

Explanation for Decrease in Spreading Rate

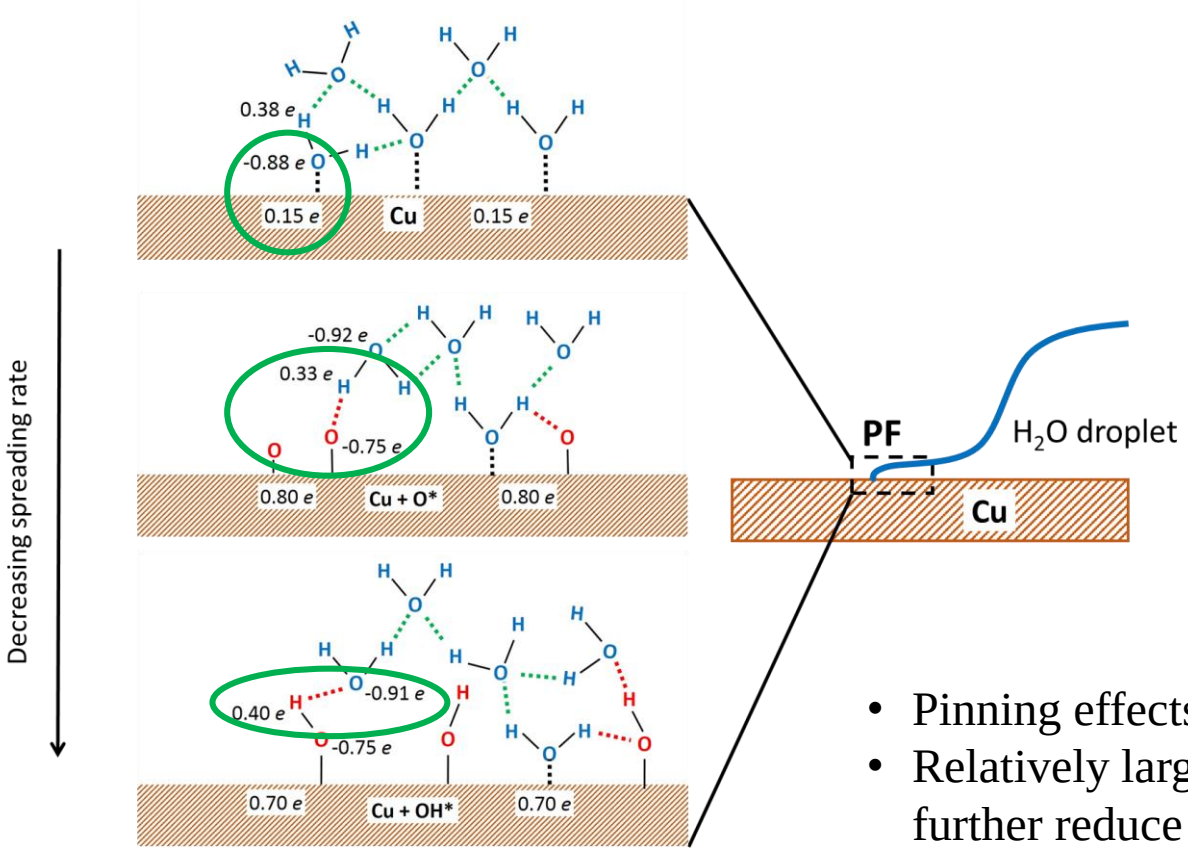

- Pinning effects of Cu-O* and Cu-OH* bonds
- Relatively larger Coulombic effects in Cu-OH* further reduce the spreading of H_2O

Antony, *et al.*, Langmuir (2016)

PennState

Summary

- COMB3 potentials can describe charge transfer between water and metal surface. Description of liquid water is reasonably good.
- Chemical nature of the surface influences the kinetics of water spreading

PennState